

Supporting Materials for

Effect of subtle changes of isomeric ligands on the
synthesis of atomically precise water-soluble gold
nanoclusters

*Xinlei Zhang,^a Ziping Wang,^b Shuyu Qian,^a Naiwei Liu,^a Lina Sui^{*a} and Xun Yuan^{*a}*

^aSchool of Materials Science and Engineering, Qingdao University of Science and
Technology, Qingdao 266042, P. R. China. Email: yuanxun@qust.edu.cn;
linasui@qust.edu.cn

^bWeifang University of Science and Technology, Shandong Peninsula Engineering
Research Center of Comprehensive Brine Utilization, Weifang 262700, P. R. China.

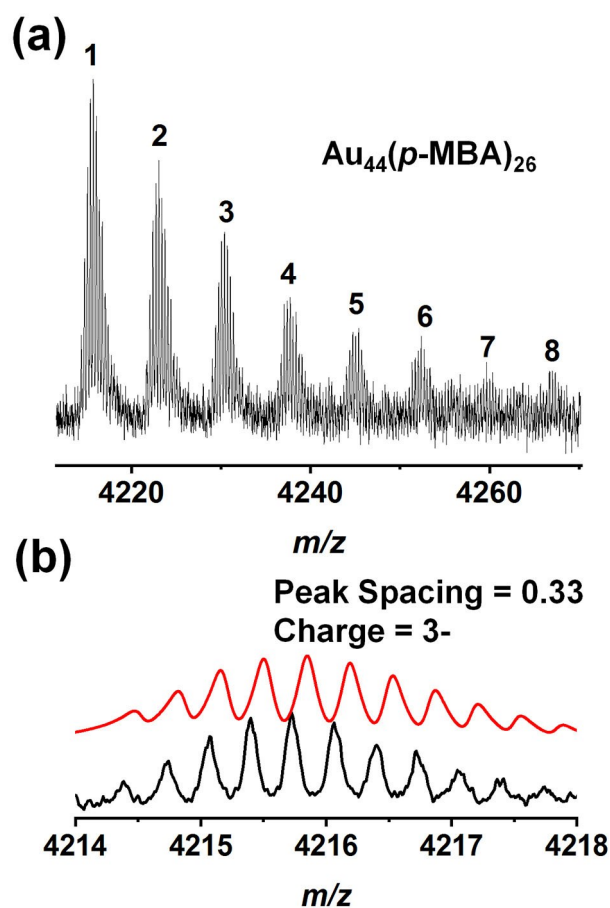


Figure S1. (a) Zoom-in ESI mass spectrum of the as-synthesized $\text{Au}_{44}(\text{p-MBA})_{26}$ NCs. (b) Isotope patterns of $[\text{Au}_{44}(\text{p-MBA})_{26}\text{-H}]^{3-}$ species acquired experimentally (black curve) and theoretically (red curve). In Figure S1a, peak #1 corresponds to $[\text{Au}_{44}(\text{p-MBA})_{26}\text{-H}]^{3-}$, and the other peaks (#2-#8) are from the successive coordination of $[\text{Na} - \text{H}]$ of peak #1.

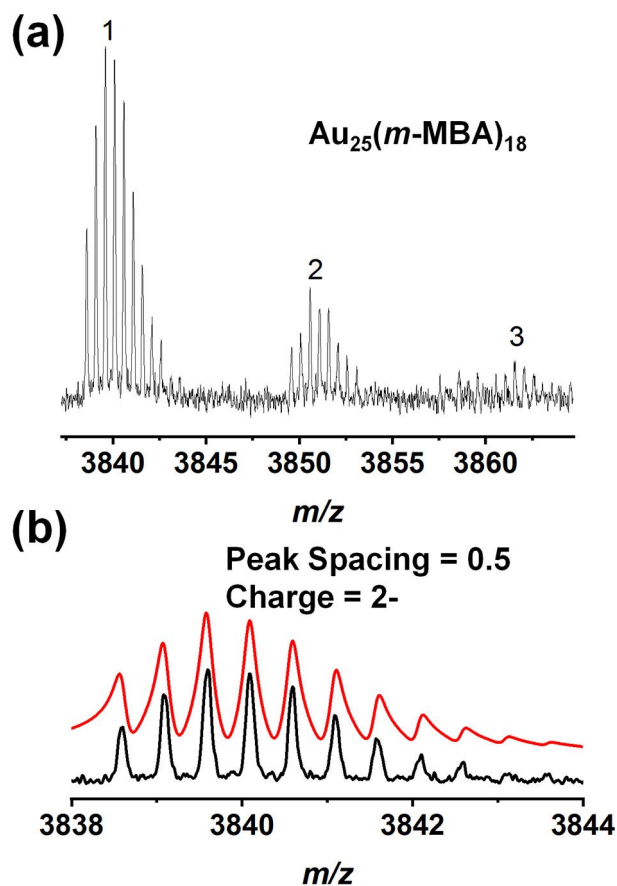


Figure S2. (a) Zoom-in ESI mass spectrum of the as-synthesized $\text{Au}_{25}(\text{m-MBA})_{18}$ NCs. (b) Isotope patterns of $[\text{Au}_{25}(\text{m-MBA})_{18}\text{-H}]^{2-}$ species acquired experimentally (black curve) and theoretically (red curve). In Figure S2a, peak #1 corresponds to $[\text{Au}_{25}(\text{m-MBA})_{18}\text{-H}]^{2-}$, and the other peaks (#2-#3) are from the successive coordination of $[\text{Na} - \text{H}]$ of peak #1.

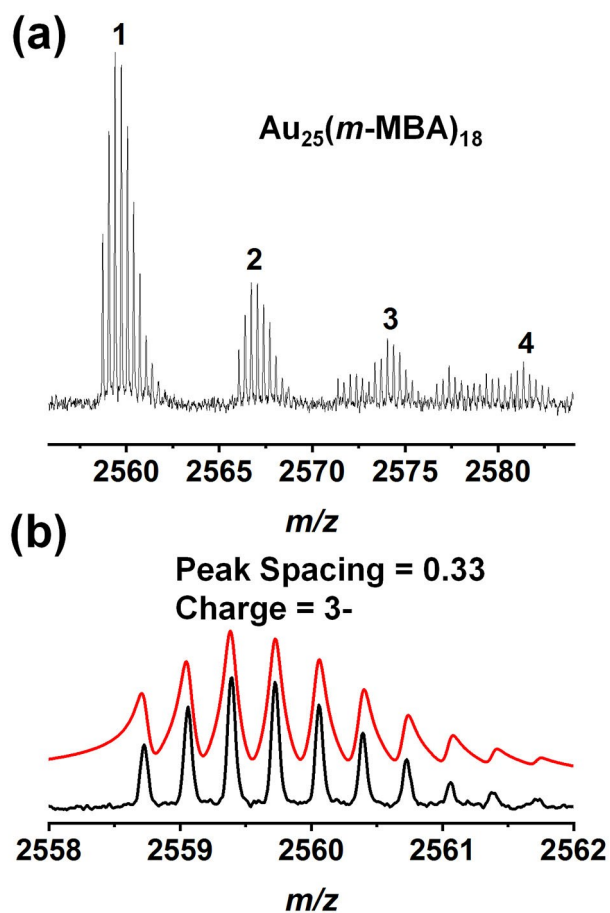


Figure S3. (a) Zoom-in ESI mass spectrum of the as-synthesized $\text{Au}_{25}(\text{m-MBA})_{18}$ NCs. (b) Isotope patterns acquired experimentally (black curve) and theoretically (red curve) for the species $[\text{Au}_{25}(\text{m-MBA})_{18}-2\text{H}]^{3-}$. In Figure S3a, peak #1 corresponds to $[\text{Au}_{25}(\text{m-MBA})_{18}-2\text{H}]^{3-}$, and the other peaks (#2-#4) are from the successive coordination of $[\text{Na} - \text{H}]$ of peak #1.

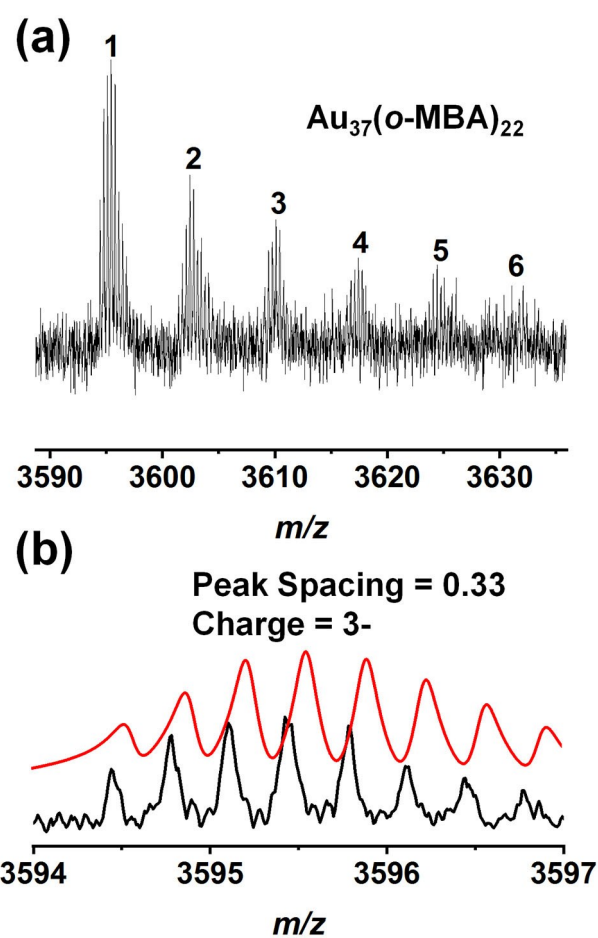


Figure S4. (a) Zoom-in ESI mass spectrum of the as-synthesized $\text{Au}_{37}(\text{o-MBA})_{22}$ NCs. (b) Isotope patterns of $[\text{Au}_{37}(\text{o-MBA})_{22}-8\text{H}+6\text{Na}]^{3-}$ species acquired experimentally (black curve) and theoretically (red curve). In Figure S4a, peak #1 corresponds to $[\text{Au}_{37}(\text{o-MBA})_{22}-8\text{H}+6\text{Na}]^{3-}$, and the other peaks (#2-#6) are from the successive coordination of $[+\text{Na} - \text{H}]$ of peak #1.

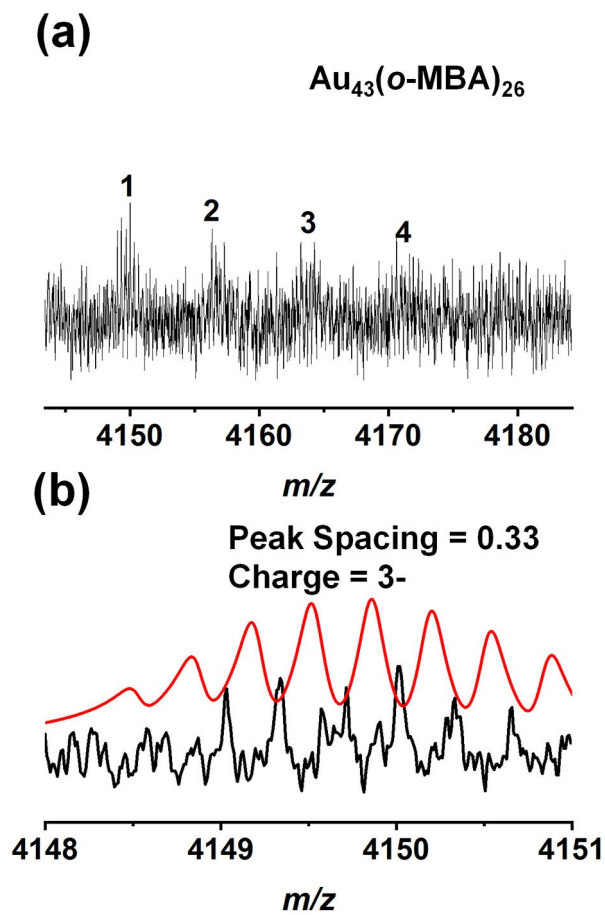


Figure S5. (a) Zoom-in ESI mass spectrum of the as-synthesized $\text{Au}_{43}(\text{o-MBA})_{26}$ NCs. (b) Isotope patterns of $[\text{Au}_{43}(\text{o-MBA})_{26}-2\text{H}]^{3-}$ species acquired experimentally (black curve) and theoretically (red curve). In Figure S5a, peak #1 corresponds to $[\text{Au}_{43}(\text{o-MBA})_{26}-2\text{H}]^{3-}$, and the other peaks (#2-#4) are from the successive coordination of $[\text{Na} - \text{H}]$ of peak #1.

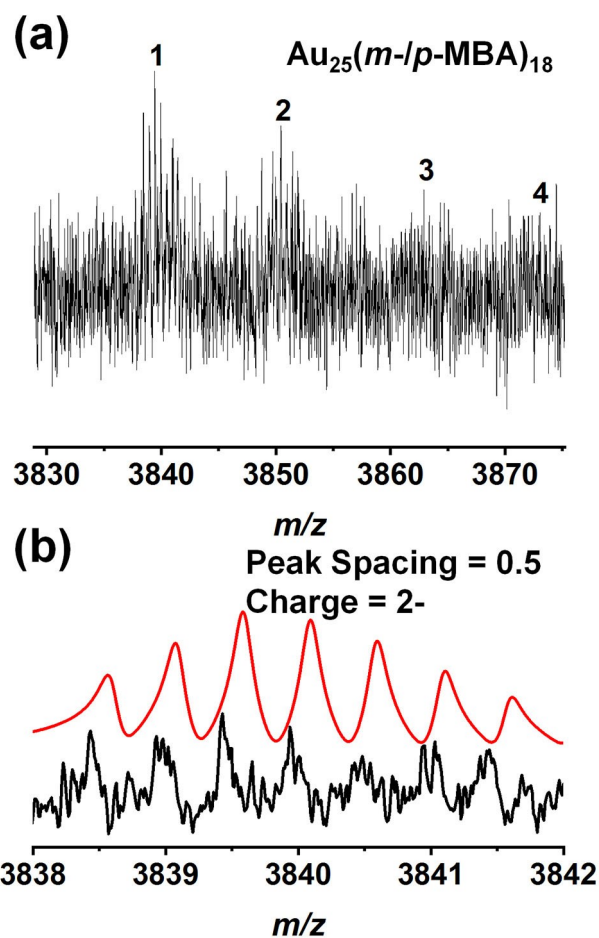


Figure S6. (a) Zoom-in ESI mass spectrum of the as-synthesized $\text{Au}_{25}(\text{m-}i>p\text{-MBA})_{18}$ NCs. (b) Isotope patterns of $[\text{Au}_{25}(\text{m-}i>p\text{-MBA})_{18}\text{-H}]^{2-}$ species acquired experimentally (black curve) and theoretically (red curve). In Figure S6a, peak #1 corresponds to $[\text{Au}_{25}(\text{m-}i>p\text{-MBA})_{18}\text{-H}]^{2-}$, and the other peaks (#2-#4) are from the successive coordination of $[+ \text{Na} - \text{H}]$ of peak #1.

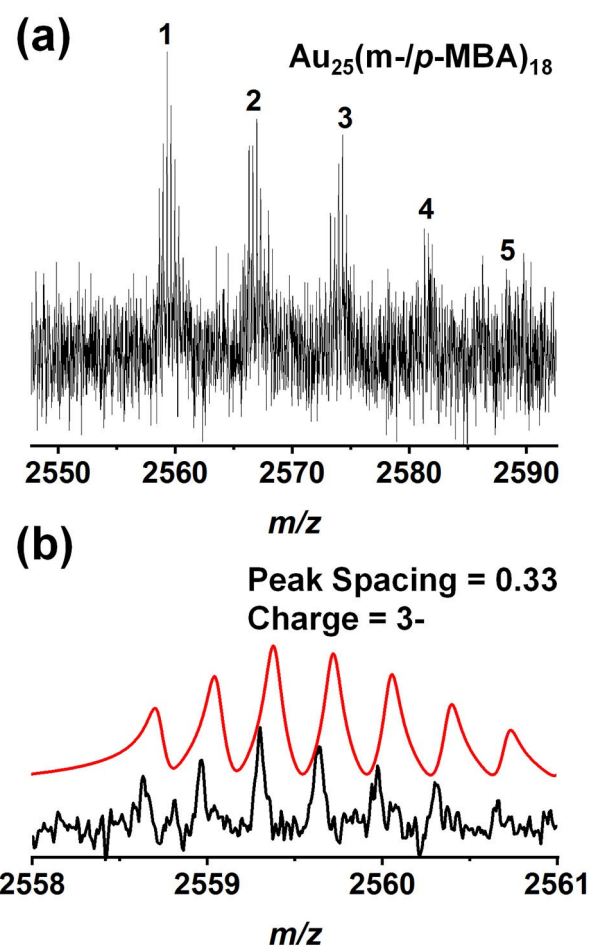


Figure S7. (a) Zoom-in ESI mass spectrum of the as-synthesized $\text{Au}_{25}(\text{m-/p-MBA})_{18}$ NCs. (b) Isotope patterns of $[\text{Au}_{25}(\text{m-/p-MBA})_{18}-2\text{H}]^{3-}$ species acquired experimentally (black curve) and theoretically (red curve). In Figure S7a, peak #1 corresponds to $[\text{Au}_{25}(\text{m-/p-MBA})_{18}-2\text{H}]^{3-}$, and the other peaks (#2-#5) are from the successive coordination of $[+\text{Na} - \text{H}]$ of peak #1.

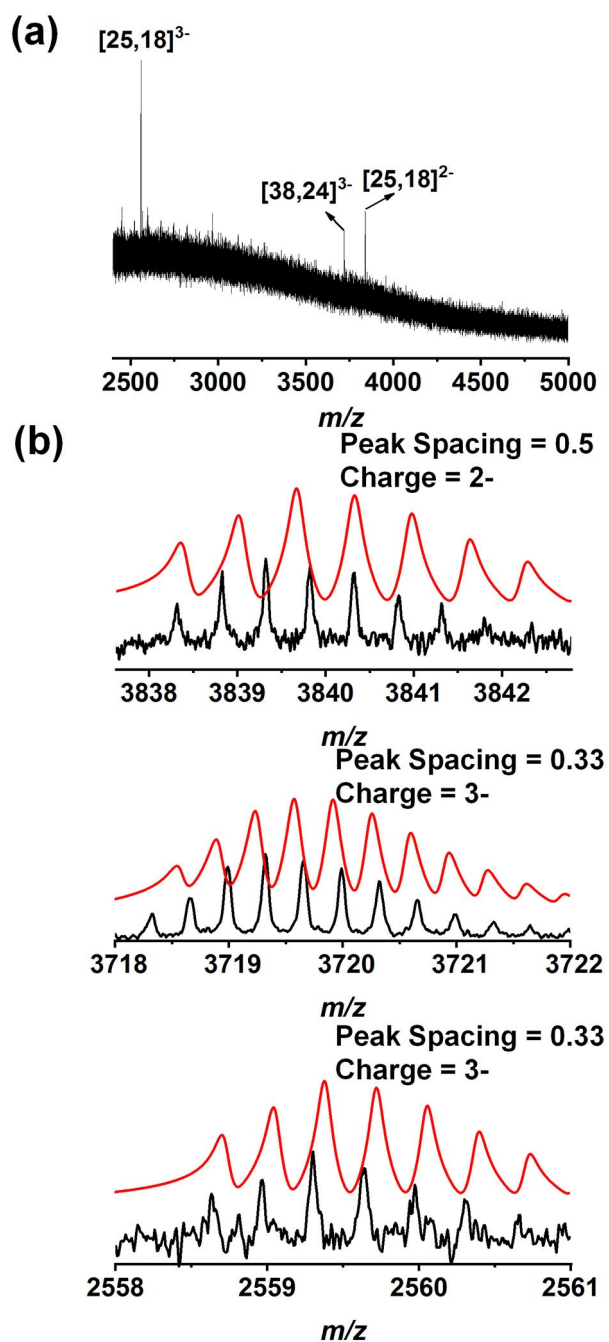


Figure S8. (a) ESI mass spectrum of $\text{Au}_{25/38}(\text{m-}/\text{p-MBA})_{18/24}$ NCs synthesized with the feeding ratio of $\text{m-MBA} : \text{p-MBA} = 1 : 2.5$. (b) Isotope patterns of $[\text{Au}_{25}(\text{m-}/\text{p-MBA})_{18}\text{-H}]^{2-}$ (upper item), $[\text{Au}_{38}(\text{m-}/\text{p-MBA})_{24}\text{-H}]^{3-}$ (middle item), and $[\text{Au}_{25}(\text{m-}/\text{p-MBA})_{18}\text{-2H}]^{3-}$ NCs (bottom item) acquired experimentally (black curve) and theoretically (red curve).

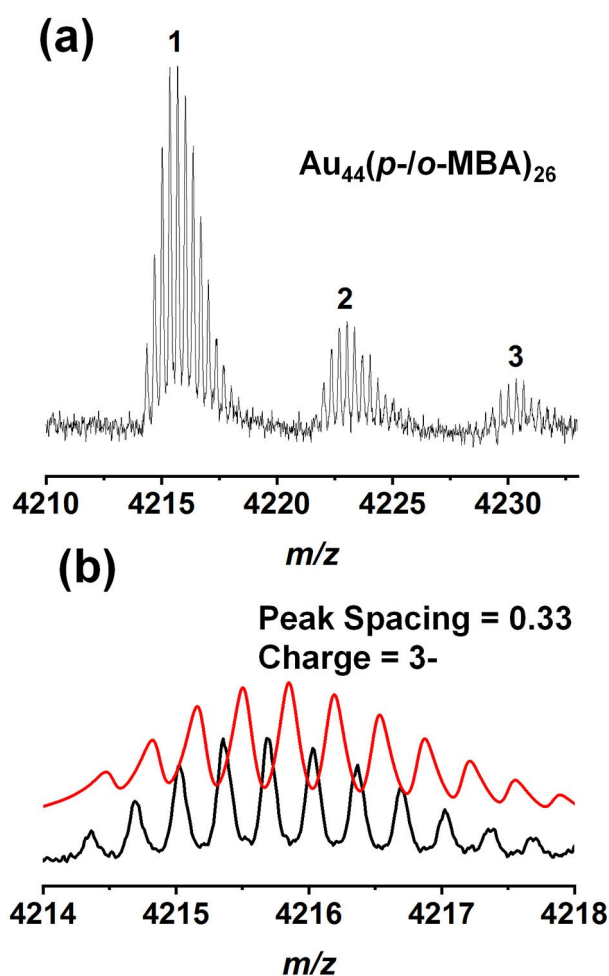


Figure S9. (a) Zoom-in ESI mass spectrum of the as-synthesized $\text{Au}_{44}(\text{p-}o\text{-MBA})_{26}$ NCs. (b) Isotope patterns of $[\text{Au}_{44}(\text{p-}o\text{-MBA})_{26}\text{-H}]^{3-}$ species acquired experimentally (black curve) and theoretically (red curve). In Figure S9a, peak #1 corresponds to $[\text{Au}_{44}(\text{p-}o\text{-MBA})_{26}\text{-H}]^{3-}$, and the other peaks (#2-#3) are from the successive coordination of $[+\text{Na} - \text{H}]$ of peak #1.

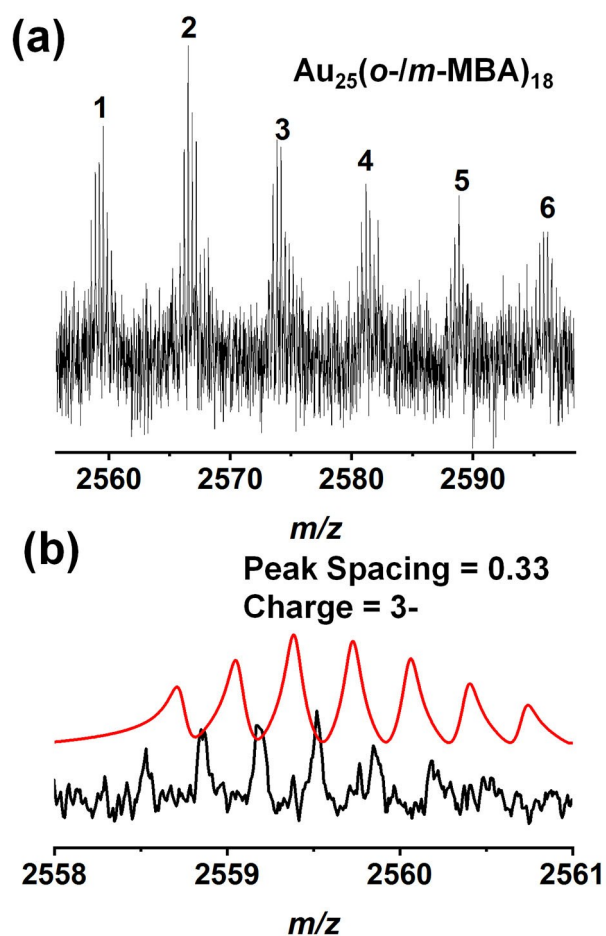


Figure S10. (a) Zoom-in ESI mass spectrum of the as-synthesized $\text{Au}_{25}(\text{o-}/\text{m-MBA})_{18}$ NCs. (b) Isotope patterns of $[\text{Au}_{25}(\text{o-}/\text{m-MBA})_{18}-2\text{H}]^{3-}$ species acquired experimentally (black curve) and theoretically (red curve). In Figure S10a, peak #1 corresponds to $[\text{Au}_{25}(\text{o-}/\text{m-MBA})_{18}-2\text{H}]^{3-}$, and the other peaks (#2-#6) are from the successive coordination of [+ Na - H] of peak #1.

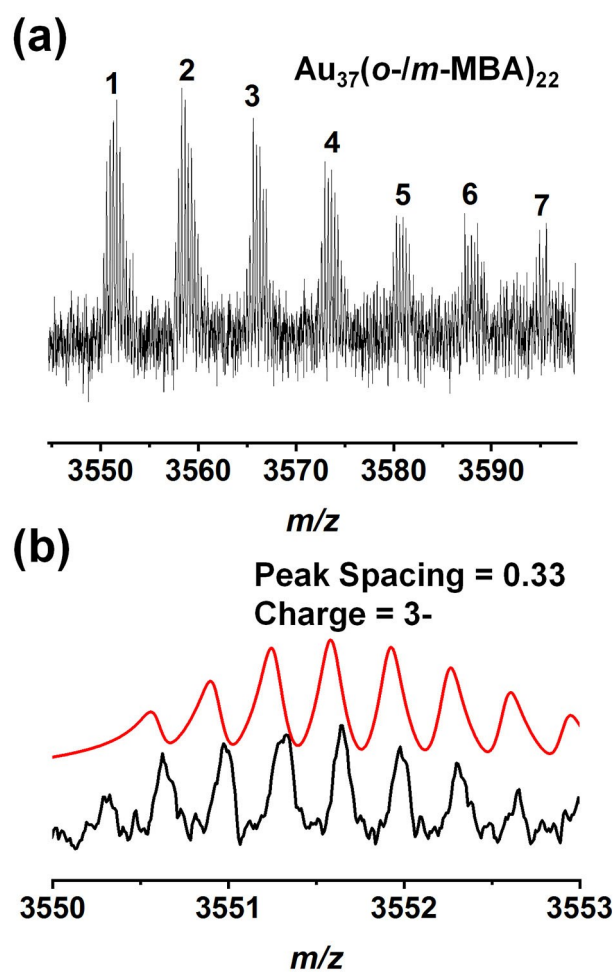


Figure S11. (a) Zoom-in ESI mass spectrum of the as-synthesized $\text{Au}_{37}(\text{o-}/\text{m-MBA})_{22}$ NCs. (b) Isotope patterns of $[\text{Au}_{37}(\text{o-}/\text{m-MBA})_{22}-2\text{H}]^{3-}$ species acquired experimentally (black curve) and theoretically (red curve). In Figure S11a, peak #1 corresponds to $[\text{Au}_{37}(\text{o-}/\text{m-MBA})_{22}-2\text{H}]^{3-}$, and the other peaks (#2-#7) are from the successive coordination of $[+\text{Na} - \text{H}]$ of peak #1.

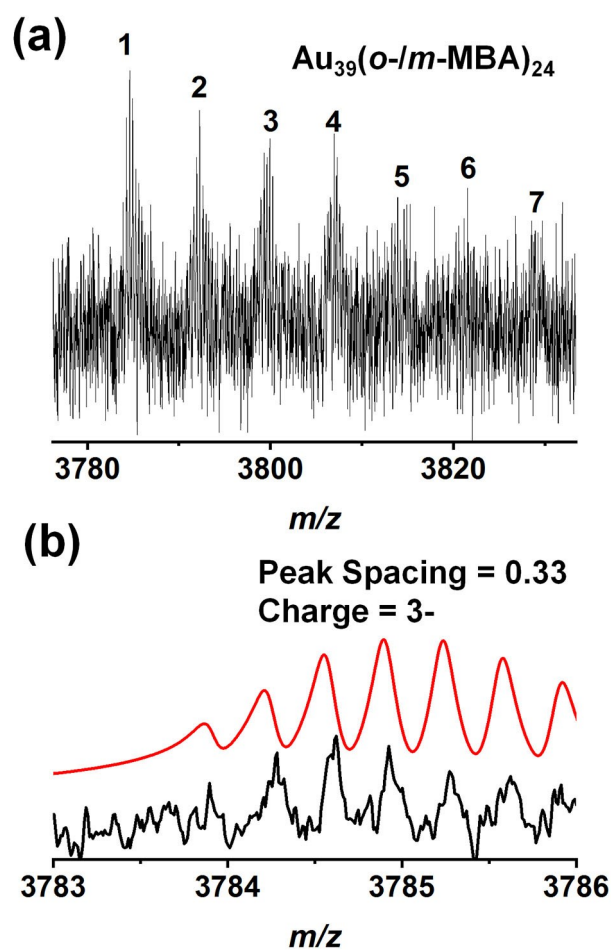


Figure S12. (a) Zoom-in ESI mass spectrum of the as-synthesized $\text{Au}_{39}(\text{o-/m-MBA})_{24}$ NCs. (b) Isotope patterns of $[\text{Au}_{39}(\text{o-/m-MBA})_{24}-2\text{H}]^{3-}$ species acquired experimentally (black curve) and theoretically (red curve). In Figure S12a, peak #1 corresponds to $[\text{Au}_{39}(\text{o-/m-MBA})_{24}-2\text{H}]^{3-}$, and the other peaks (#2-#7) are from the successive coordination of $[+\text{Na} - \text{H}]$ of peak #1.

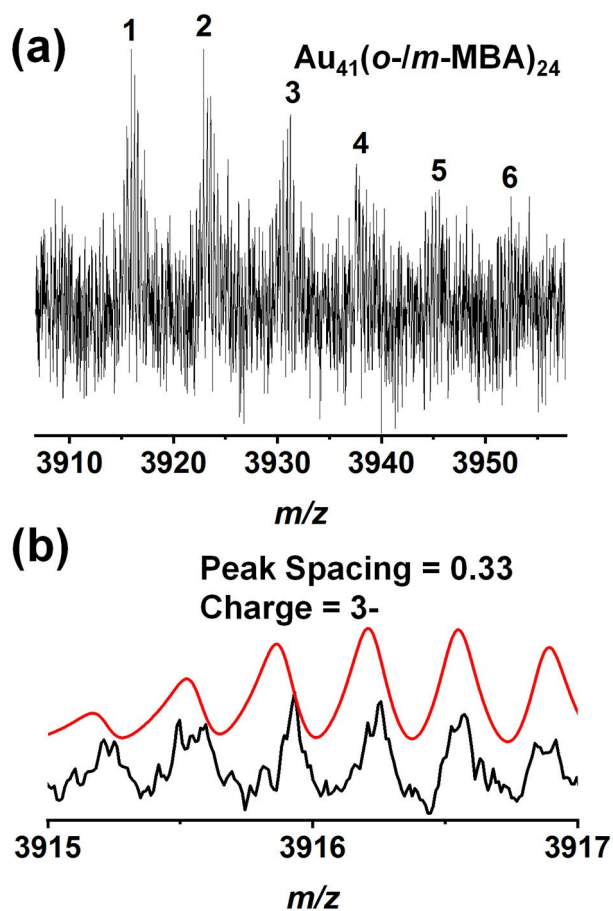


Figure S13. (a) Zoom-in ESI mass spectrum of the as-synthesized $\text{Au}_{41}(\text{o-/m-MBA})_{24}$ NCs. (b) Isotope patterns of $[\text{Au}_{41}(\text{o-/m-MBA})_{24}-2\text{H}]^{3-}$ species acquired experimentally (black curve) and theoretically (red curve). In Figure S13a, peak #1 corresponds to $[\text{Au}_{41}(\text{o-/m-MBA})_{24}-2\text{H}]^{3-}$, and the other peaks (#2-#6) are from the successive coordination of $[+\text{Na} - \text{H}]$ of peak #1.

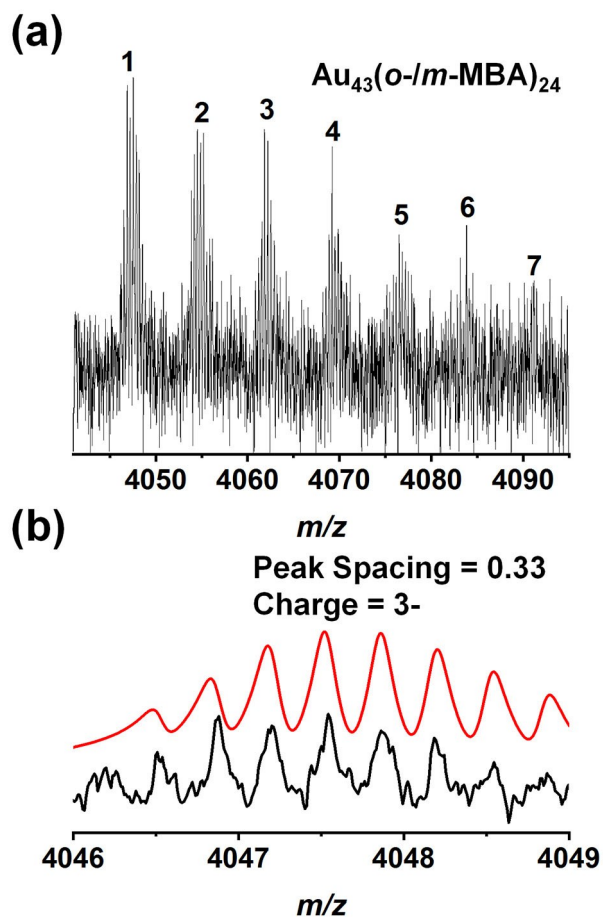
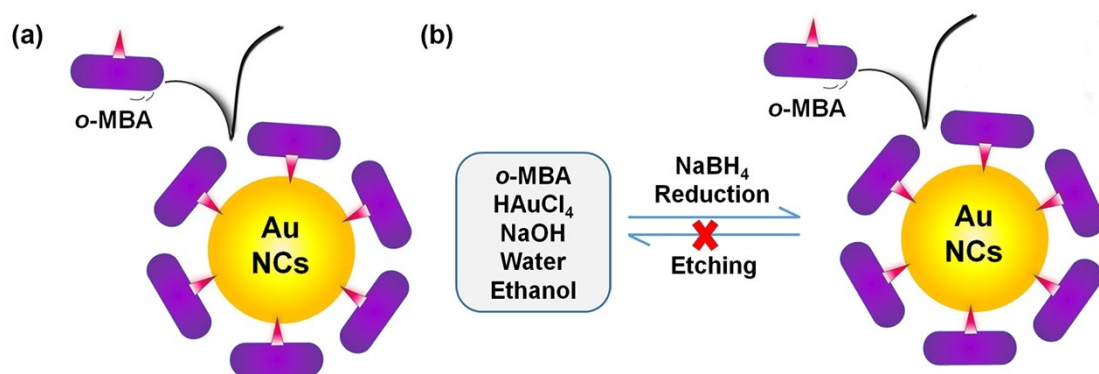


Figure S14. (a) Zoom-in ESI mass spectrum of the as-synthesized $\text{Au}_{43}(\text{o-}/\text{m-MBA})_{24}$ NCs. (b) Isotope patterns of $[\text{Au}_{43}(\text{o-}/\text{m-MBA})_{24}-2\text{H}]^{3-}$ species acquired experimentally (black curve) and theoretically (red curve). In Figure S14a, peak #1 corresponds to $[\text{Au}_{43}(\text{o-}/\text{m-MBA})_{24}-2\text{H}]^{3-}$, and the other peaks (#2-#7) are from the successive coordination of $[\text{+ Na} - \text{H}]$ of peak #1.



Scheme S1. (a) Schematic illustration of the *o*-MBA protected Au NCs with the well coated *o*-MBA shell that preventing the permeation and etching of enthetic *o*-MBA molecule. (b) Schematic illustration of the synthetic process of *o*-MBA protected Au NCs. In this NaOH-mediated NaBH₄ reduction system, the synthetic process of Au NCs composes of forward reduction reactions processing Au(I) complexes to Au NCs, and backward etching reactions processing Au NCs to Au(I) complexes, which will achieve an equilibrium through continuous reactions and display a size-focusing behavior. However, owing to the larger steric hindrance of *o*-MBA molecules, the enthetic *o*-MBA molecules are unable to permeate into the MBA shell of the formed Au NCs, which made the backward etching impossible, leading to the failure in synthesizing monodisperse *o*-MBA protected Au NCs because of the prohibited size focusing process.

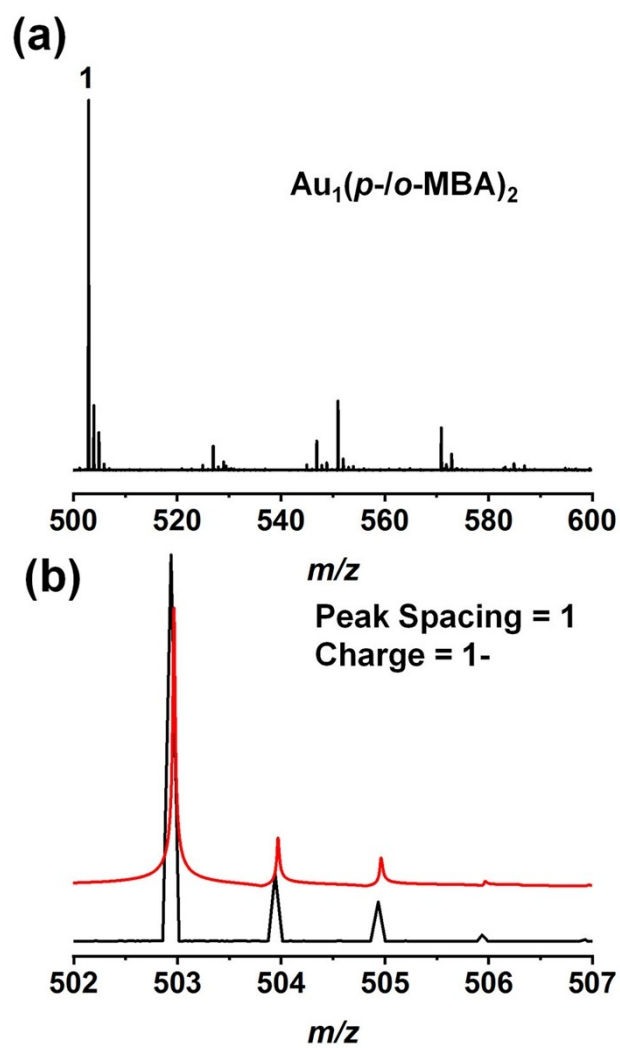


Figure S15. (a) Zoom-in ESI mass spectrum of the as-synthesized $[\text{Au}_1(p\text{-}o\text{-MBA})_2]^-$. (b) Isotope patterns of $[\text{Au}_1(p\text{-}o\text{-MBA})_2]^-$ species acquired experimentally (black curve) and theoretically (red curve).

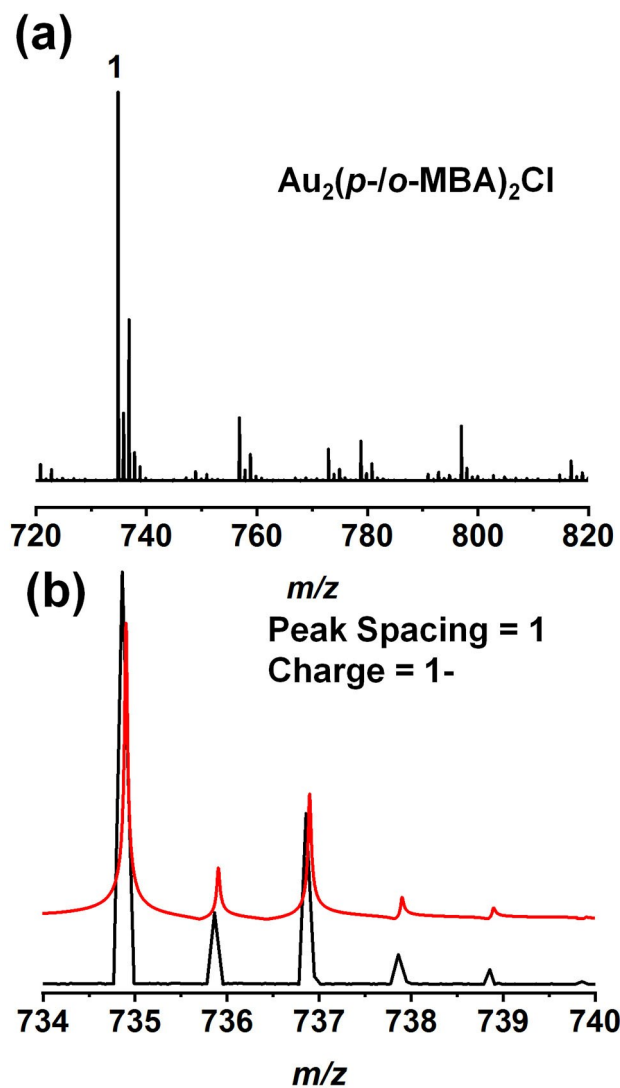


Figure S16. (a) Zoom-in ESI mass spectrum of the as-synthesized $[\text{Au}_2(p\text{-}o\text{-MBA})_2\text{Cl}]^-$. (b) Isotope patterns of $[\text{Au}_2(p\text{-}o\text{-MBA})_2\text{Cl}]^-$ species acquired experimentally (black curve) and theoretically (red curve).

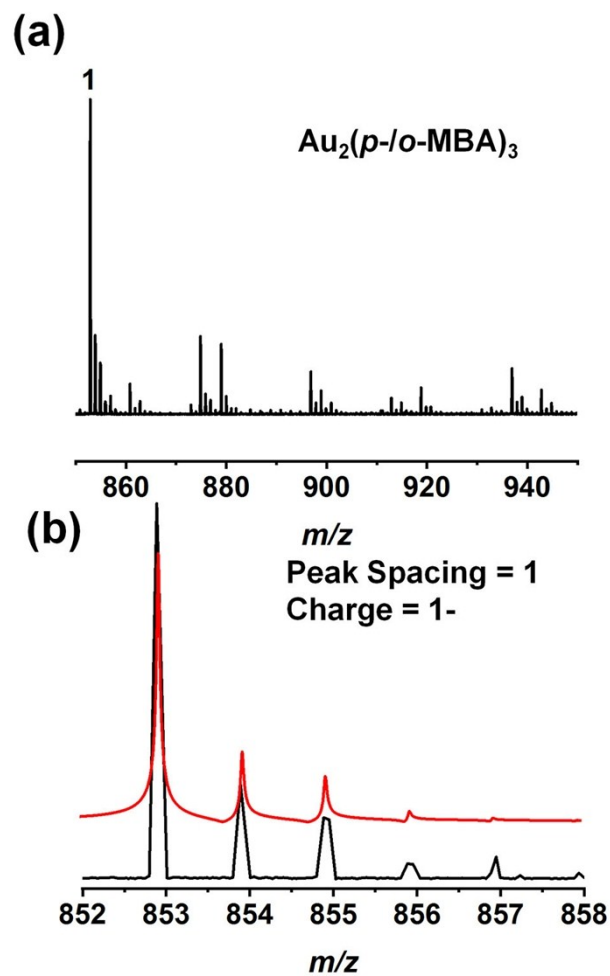


Figure S17. (a) Zoom-in ESI mass spectrum of the as-synthesized $[\text{Au}_2(p\text{-}o\text{-MBA})_3]^-$.
(b) Isotope patterns of $[\text{Au}_2(p\text{-}o\text{-MBA})_3]^-$ species acquired experimentally (black curve) and theoretically (red curve).

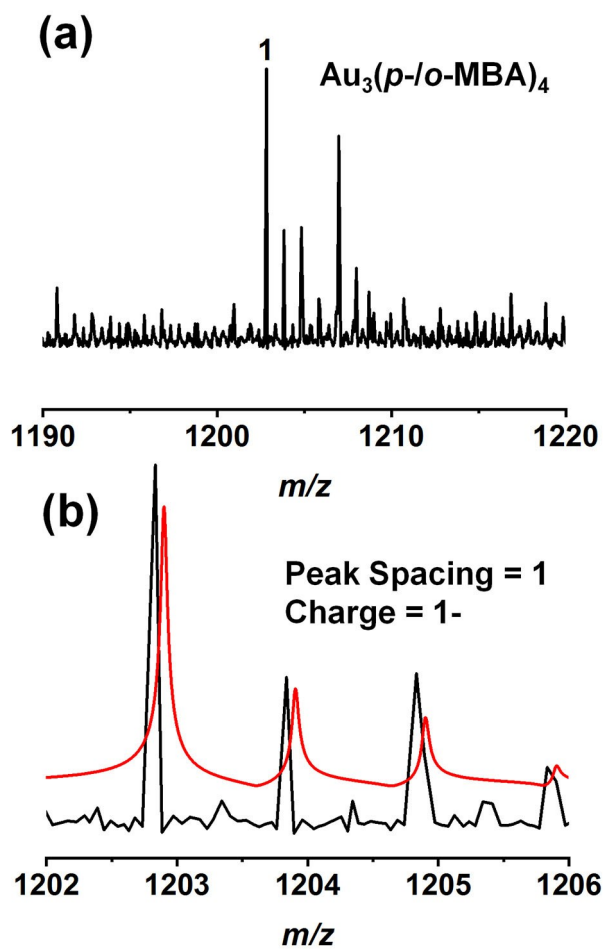


Figure S18. (a) Zoom-in ESI mass spectrum of the as-synthesized $[\text{Au}_3(p\text{-}o\text{-MBA})_4]^-$. (b) Isotope patterns of $[\text{Au}_3(p\text{-}o\text{-MBA})_4]^-$ species acquired experimentally (black curve) and theoretically (red curve).

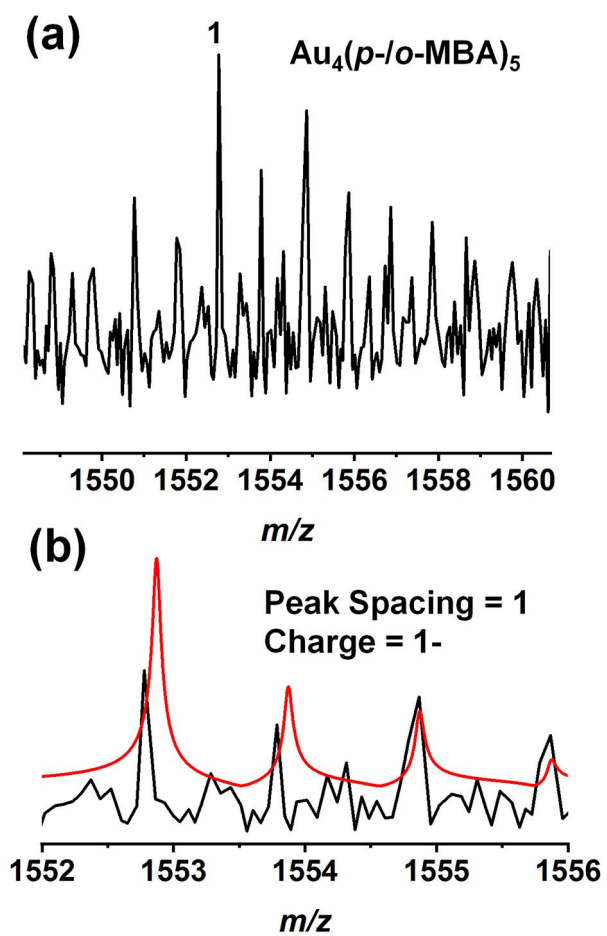


Figure S19. (a) Zoom-in ESI mass spectrum of the as-synthesized $[\text{Au}_4(p\text{-/}o\text{-MBA})_5]^-$.
(b) Isotope patterns of $[\text{Au}_4(p\text{-/}o\text{-MBA})_5]^-$ species acquired experimentally (black curve) and theoretically (red curve).

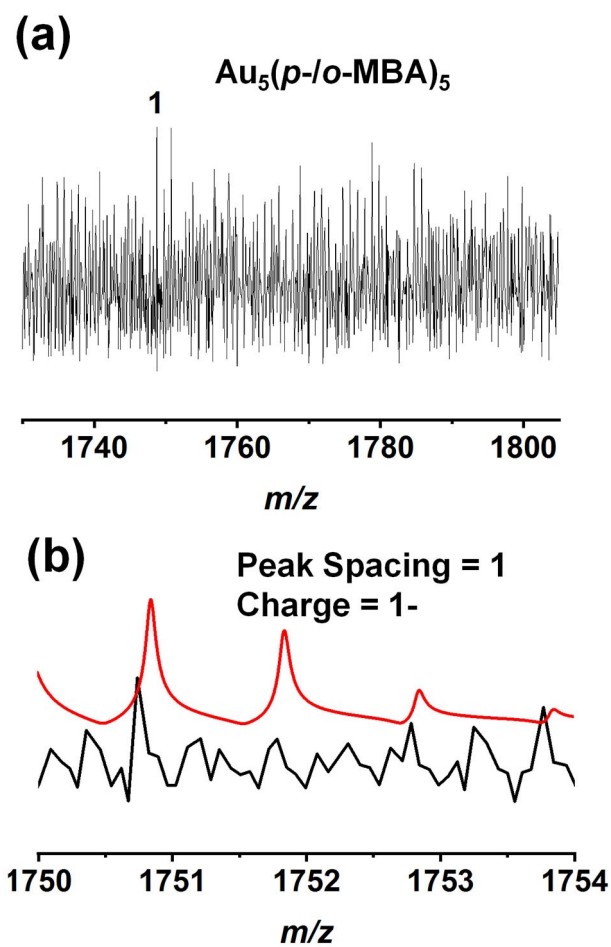


Figure S20. (a) Zoom-in ESI mass spectrum of the as-synthesized $[\text{Au}_5(p\text{-}o\text{-MBA})_5]^-$.
(b) Isotope patterns of $[\text{Au}_5(p\text{-}o\text{-MBA})_5]^-$ species acquired experimentally (black curve) and theoretically (red curve).

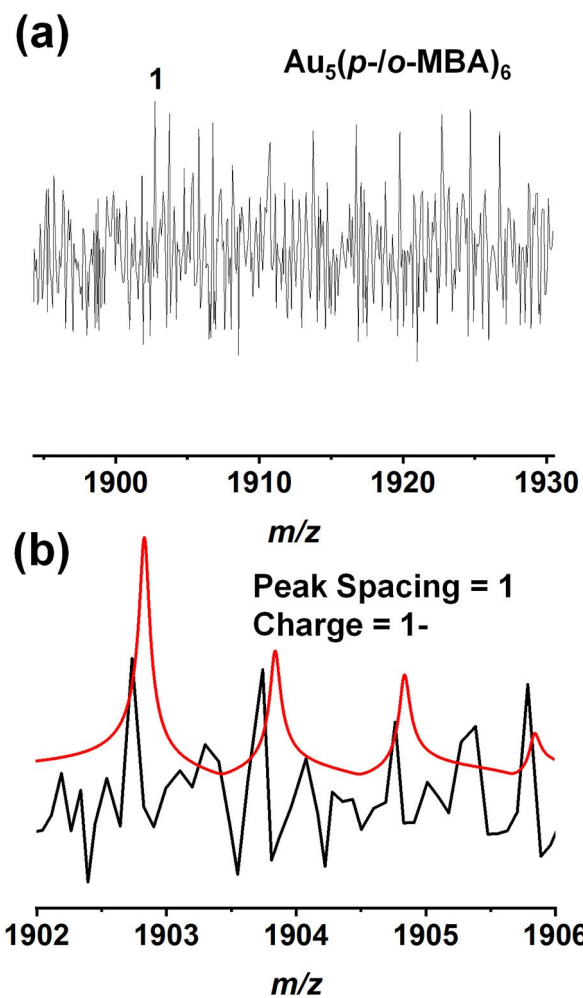


Figure S21. (a) Zoom-in ESI mass spectrum of the as-synthesized $[Au_5(p-o-MBA)_6]^-$.
(b) Isotope patterns of $[Au_5(p-o-MBA)_6]^-$ species acquired experimentally (black curve) and theoretically (red curve).

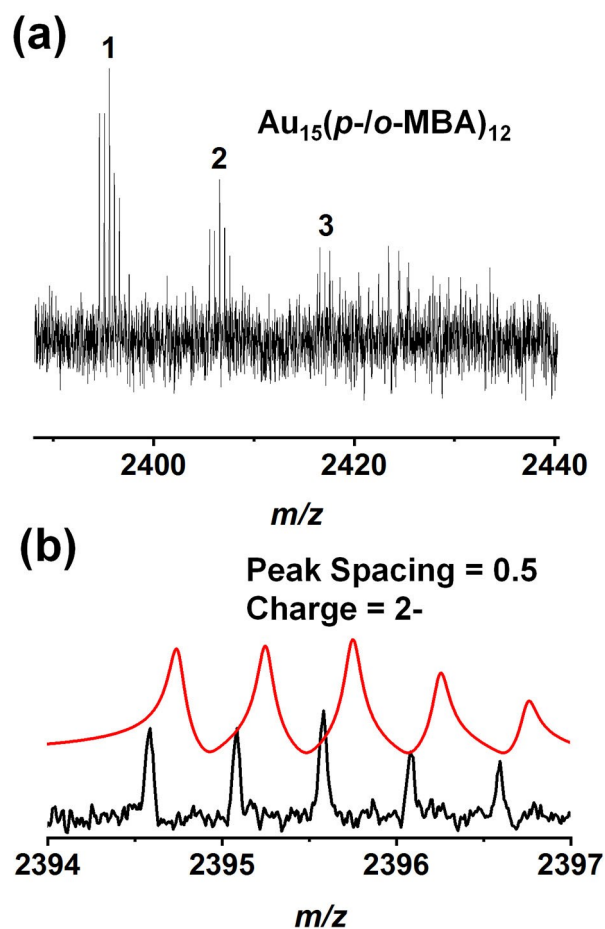


Figure S22. (a) Zoom-in ESI mass spectrum of the as-synthesized $\text{Au}_{15}(\text{p-}o\text{-MBA})_{12}$ NCs. (b) Isotope patterns of $[\text{Au}_{15}(\text{p-}o\text{-MBA})_{12}\text{-H}]^{2-}$ species acquired experimentally (black curve) and theoretically (red curve). In Figure S22a, peak #1 corresponds to $[\text{Au}_{15}(\text{p-}o\text{-MBA})_{12}\text{-H}]^{2-}$, and the other peaks (#2-#3) are from the successive coordination of $[+\text{Na} - \text{H}]$ of peak #1.

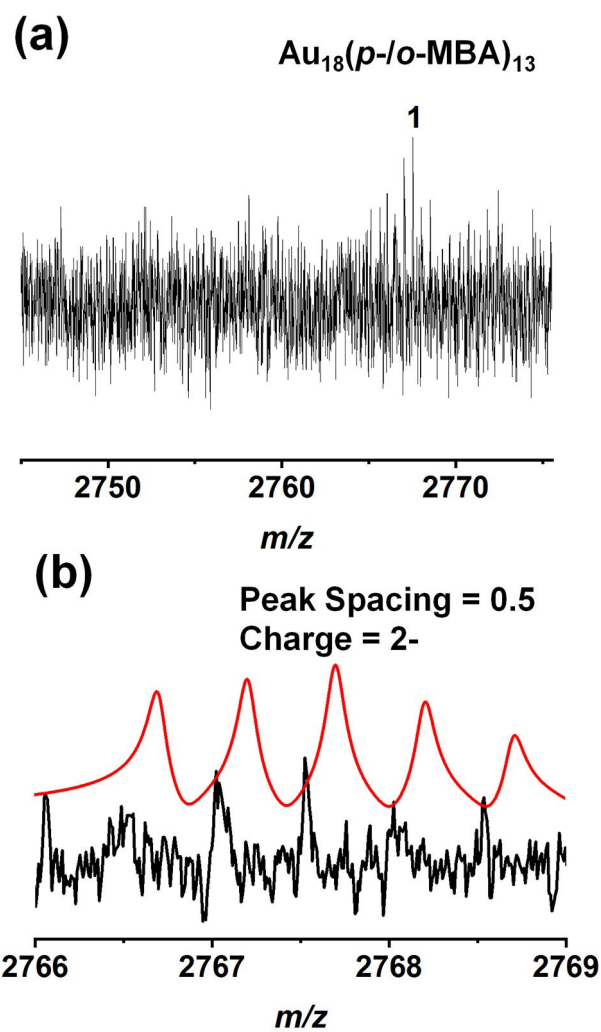


Figure S23. (a) Zoom-in ESI mass spectrum of the as-synthesized $\text{Au}_{18}(\text{p-}o\text{-MBA})_{13}$ NCs. (b) Isotope patterns of $[\text{Au}_{18}(\text{p-}o\text{-MBA})_{13}\text{-H}]^{2-}$ species acquired experimentally (black curve) and theoretically (red curve).

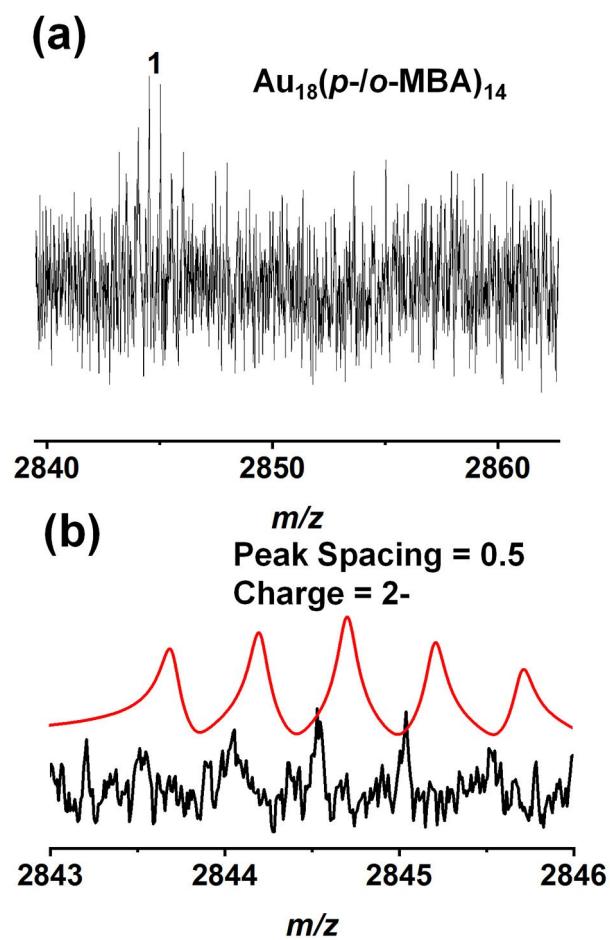


Figure S24. (a) Zoom-in ESI mass spectrum of the as-synthesized $\text{Au}_{18}(\text{p-}o\text{-MBA})_{14}$ NCs. (b) Isotope patterns of $[\text{Au}_{18}(\text{p-}o\text{-MBA})_{14}]^{2-}$ species acquired experimentally (black curve) and theoretically (red curve).

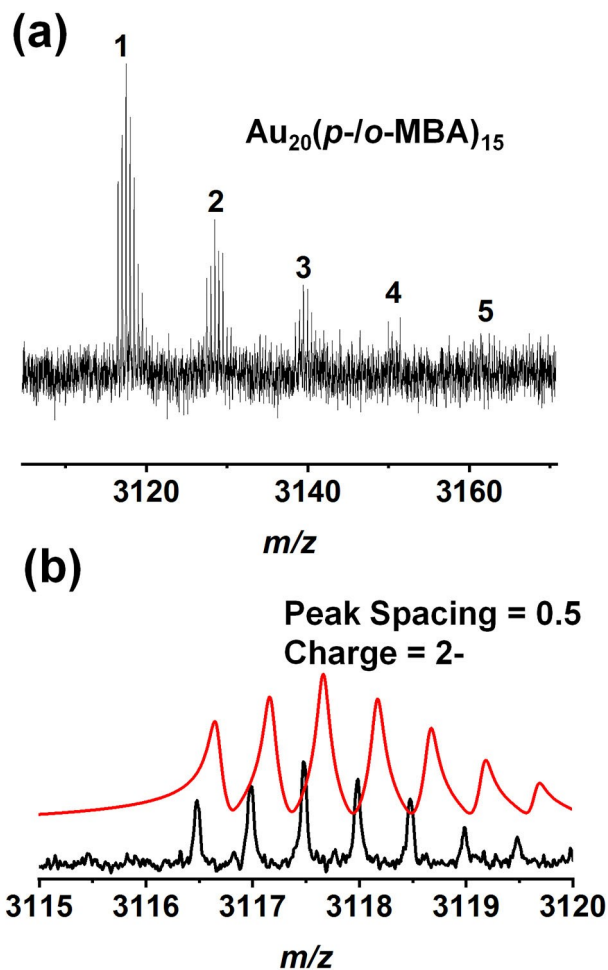


Figure S25. (a) Zoom-in ESI mass spectrum of the as-synthesized $\text{Au}_{20}(\text{p-}o\text{-MBA})_{15}$ NCs. (b) Isotope patterns of $[\text{Au}_{20}(\text{p-}o\text{-MBA})_{15}\text{-H}]^{2-}$ species acquired experimentally (black curve) and theoretically (red curve). In Figure S25a, peak #1 corresponds to $[\text{Au}_{20}(\text{p-}o\text{-MBA})_{15}\text{-H}]^{2-}$, and the other peaks (#2-#5) are from the successive coordination of $[+\text{Na} - \text{H}]$ of peak #1.

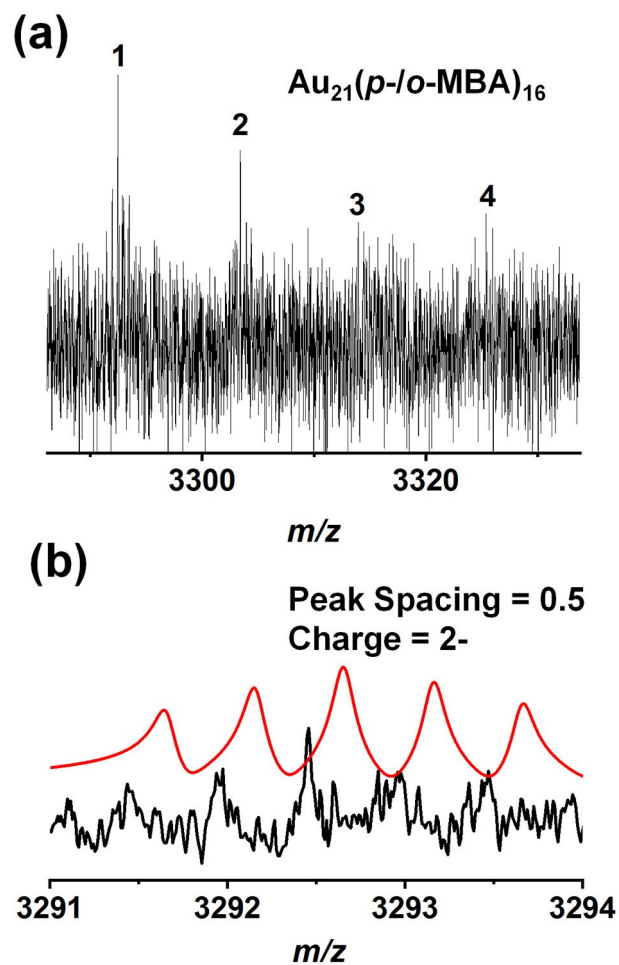


Figure S26. (a) Zoom-in ESI mass spectrum of the as-synthesized $\text{Au}_{21}(\text{p-}o\text{-MBA})_{16}$ NCs. (b) Isotope patterns of $[\text{Au}_{21}(\text{p-}o\text{-MBA})_{16}\text{-H}]^{2-}$ species acquired experimentally (black curve) and theoretically (red curve). In Figure S26a, peak #1 corresponds to $[\text{Au}_{21}(\text{p-}o\text{-MBA})_{16}\text{-H}]^{2-}$, and the other peaks (#2-#4) are from the successive coordination of $[+\text{Na} - \text{H}]$ of peak #1.

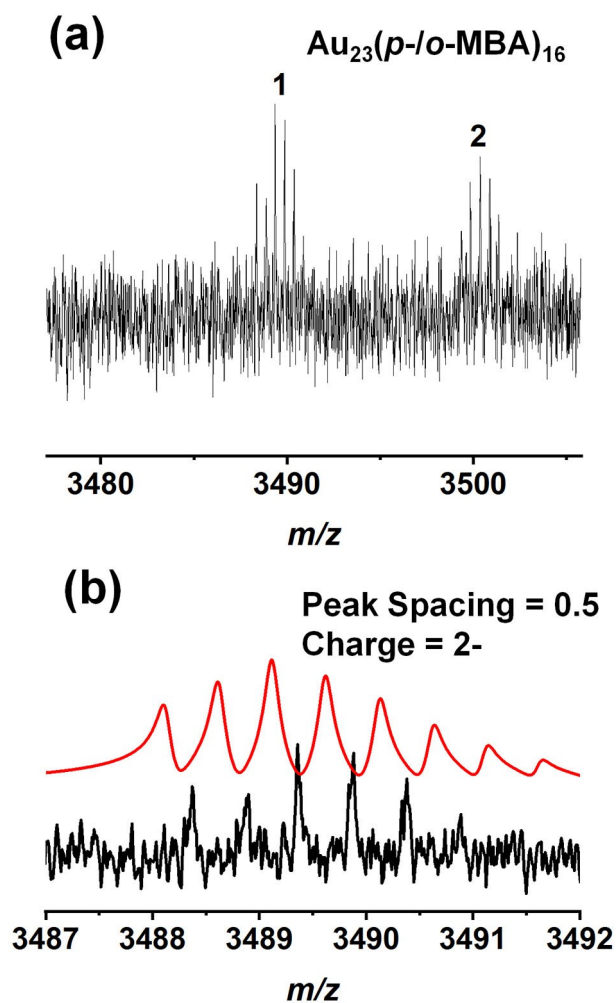


Figure S27. (a) Zoom-in ESI mass spectrum of the as-synthesized $\text{Au}_{23}(\text{p-}o\text{-MBA})_{16}$ NCs. (b) Isotope patterns of $[\text{Au}_{23}(\text{p-}o\text{-MBA})_{16}\text{-H}]^{2-}$ species acquired experimentally (black curve) and theoretically (red curve). In Figure S27a, peak #1 corresponds to $[\text{Au}_{23}(\text{p-}o\text{-MBA})_{16}\text{-H}]^{2-}$, and the other peaks (#2) are from the successive coordination of $[+\text{Na} - \text{H}]$ of peak #1.

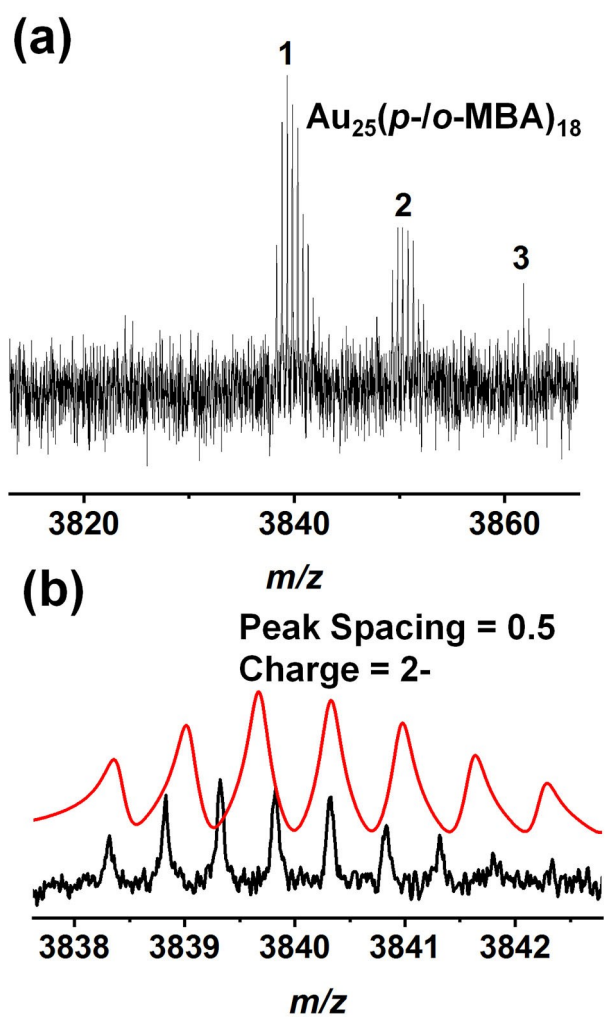


Figure S28. (a) Zoom-in ESI mass spectrum of the as-synthesized $\text{Au}_{25}(\text{p-}o\text{-MBA})_{18}$ NCs. (b) Isotope patterns of $[\text{Au}_{25}(\text{p-}o\text{-MBA})_{18}\text{-H}]^{2-}$ species acquired experimentally (black curve) and theoretically (red curve). In Figure S28a, peak #1 corresponds to $[\text{Au}_{25}(\text{p-}o\text{-MBA})_{18}\text{-H}]^{2-}$, and the other peaks (#2-#3) are from the successive coordination of $[+\text{Na} - \text{H}]$ of peak #1.

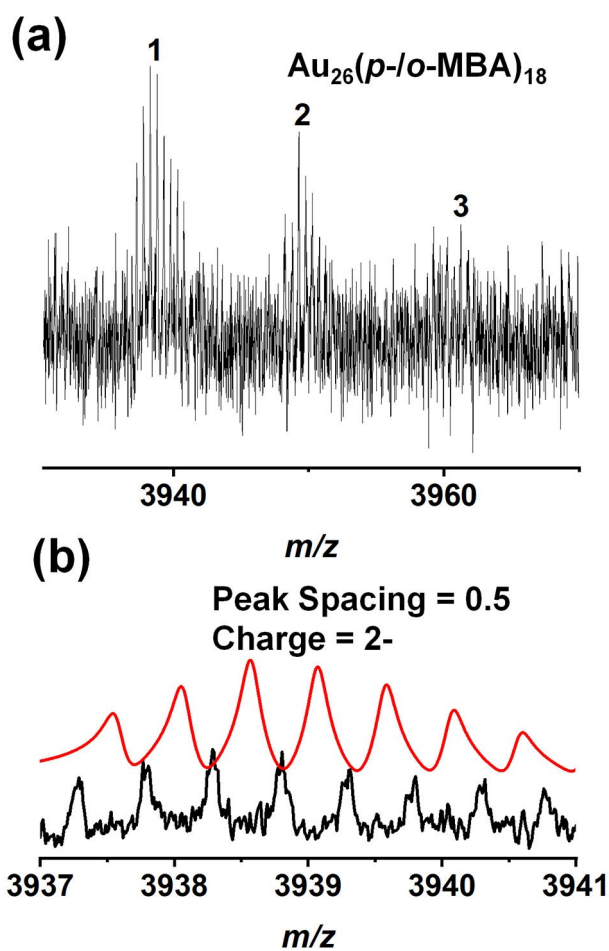


Figure S29. (a) Zoom-in ESI mass spectrum of the as-synthesized $\text{Au}_{26}(\text{p-}o\text{-MBA})_{18}$ NCs. (b) Isotope patterns of $[\text{Au}_{26}(\text{p-}o\text{-MBA})_{18}]^{2-}$ species acquired experimentally (black curve) and theoretically (red curve). In Figure S29a, peak #1 corresponds to $[\text{Au}_{26}(\text{p-}o\text{-MBA})_{18}]^{2-}$, and the other peaks (#2-#3) are from the successive coordination of [+ Na - H] of peak #1.

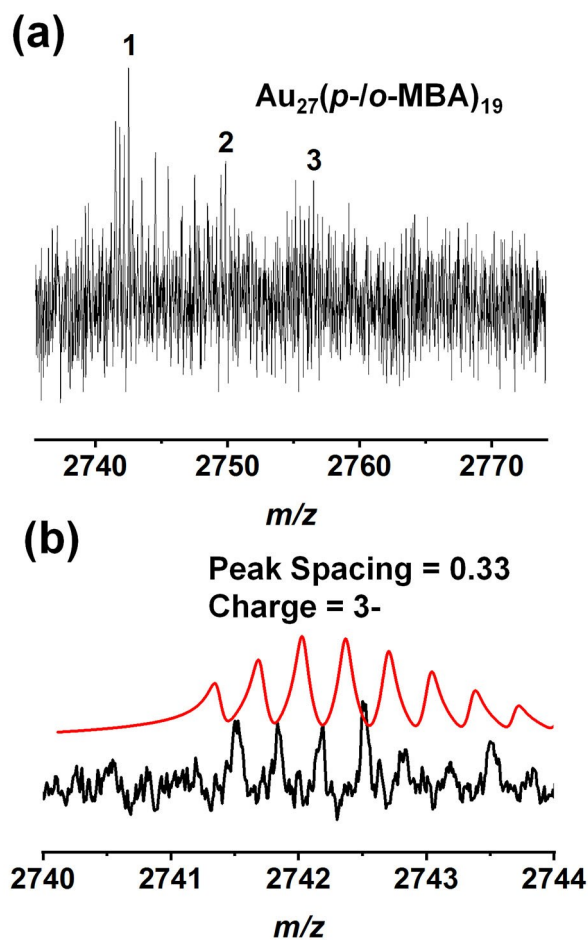


Figure S30. (a) Zoom-in ESI mass spectrum of the as-synthesized $\text{Au}_{27}(\text{p-}o\text{-MBA})_{19}$ NCs. (b) Isotope patterns of $[\text{Au}_{27}(\text{p-}o\text{-MBA})_{19}\text{-H}]^{3-}$ species acquired experimentally (black curve) and theoretically (red curve). In Figure S30a, peak #1 corresponds to $[\text{Au}_{27}(\text{p-}o\text{-MBA})_{19}\text{-H}]^{3-}$, and the other peaks (#2-#3) are from the successive coordination of $[+\text{Na} - \text{H}]$ of peak #1.

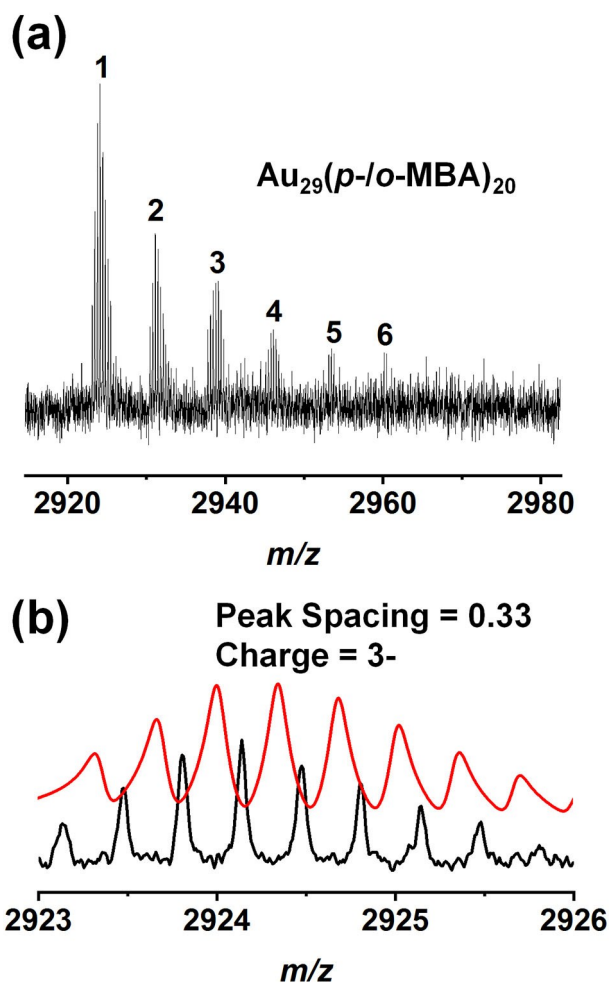


Figure S31. (a) Zoom-in ESI mass spectrum of the as-synthesized $\text{Au}_{29}(\text{p-}o\text{-MBA})_{20}$ NCs. (b) Isotope patterns of $[\text{Au}_{29}(\text{p-}o\text{-MBA})_{20}\text{-}2\text{H}]^{3-}$ species acquired experimentally (black curve) and theoretically (red curve). In Figure S31a, peak #1 corresponds to $[\text{Au}_{29}(\text{p-}o\text{-MBA})_{20}\text{-}2\text{H}]^{3-}$, and the other peaks (#2-#6) are from the successive coordination of $[+\text{Na} - \text{H}]$ of peak #1.

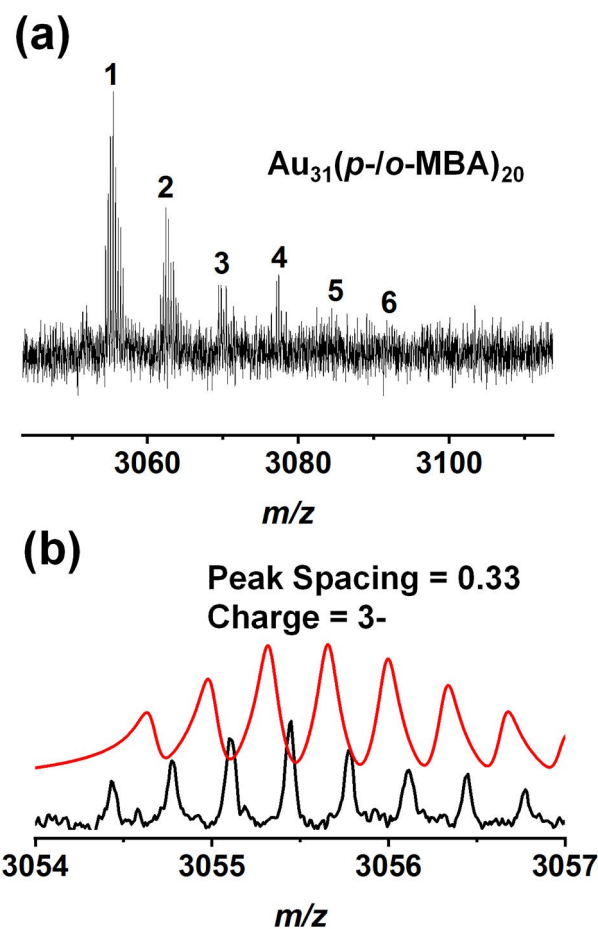


Figure S32. (a) Zoom-in ESI mass spectrum of the as-synthesized $\text{Au}_{31}(\text{p-}o\text{-MBA})_{20}$ NCs. (b) Isotope patterns of $[\text{Au}_{31}(\text{p-}o\text{-MBA})_{20}\text{-}2\text{H}]^{3-}$ species acquired experimentally (black curve) and theoretically (red curve). In Figure S32a, peak #1 corresponds to $[\text{Au}_{31}(\text{p-}o\text{-MBA})_{20}\text{-}2\text{H}]^{3-}$, and the other peaks (#2-#6) are from the successive coordination of $[+\text{Na} - \text{H}]$ of peak #1.

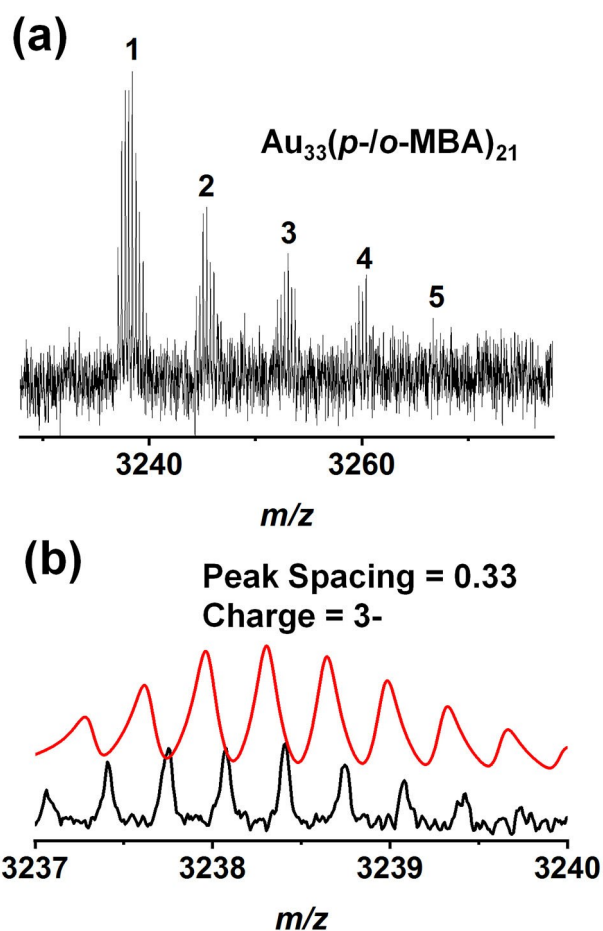


Figure S33. (a) Zoom-in ESI mass spectrum of the as-synthesized $\text{Au}_{33}(\text{p-}o\text{-MBA})_{21}$ NCs. (b) Isotope patterns of $[\text{Au}_{33}(\text{p-}o\text{-MBA})_{21}\text{-H}]^{3-}$ species acquired experimentally (black curve) and theoretically (red curve). In Figure S33a, peak #1 corresponds to $[\text{Au}_{33}(\text{p-}o\text{-MBA})_{21}\text{-H}]^{3-}$, and the other peaks (#2-#5) are from the successive coordination of $[+\text{Na} - \text{H}]$ of peak #1.

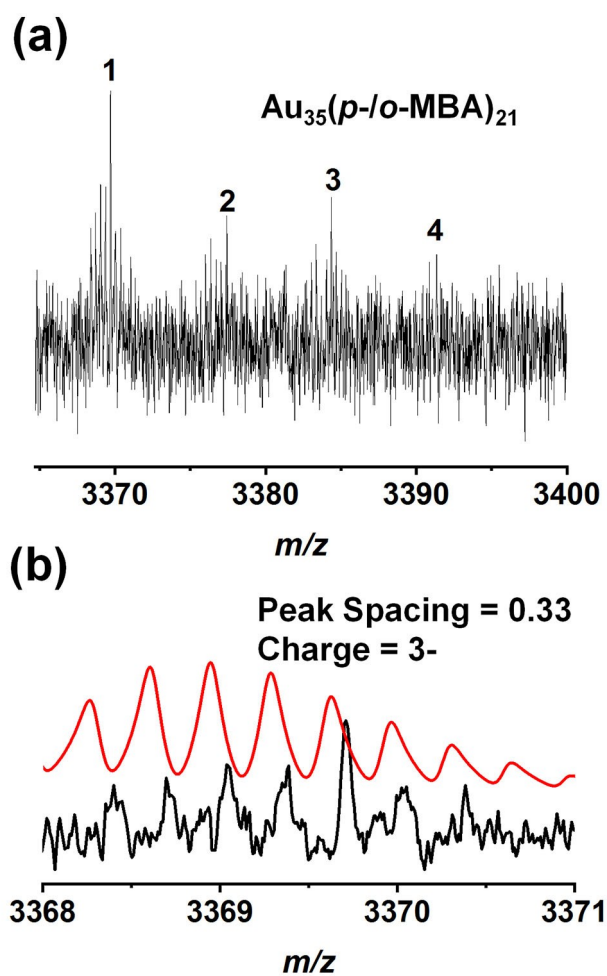


Figure S34. (a) Zoom-in ESI mass spectrum of the as-synthesized $\text{Au}_{35}(\text{p-}o\text{-MBA})_{21}$ NCs. (b) Isotope patterns of $[\text{Au}_{35}(\text{p-}o\text{-MBA})_{21}\text{-}3\text{H}]^{3-}$ species acquired experimentally (black curve) and theoretically (red curve). In Figure S34a, peak #1 corresponds to $[\text{Au}_{35}(\text{p-}o\text{-MBA})_{21}\text{-}3\text{H}]^{3-}$, and the other peaks (#2-#4) are from the successive coordination of $[+\text{Na} - \text{H}]$ of peak #1.

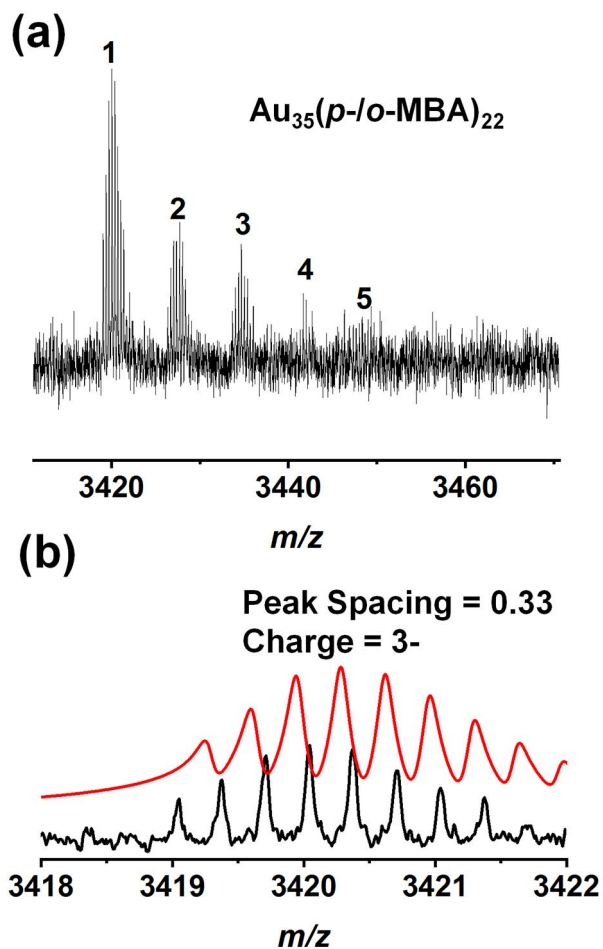


Figure S35. (a) Zoom-in ESI mass spectrum of the as-synthesized $\text{Au}_{35}(\text{p-}o\text{-MBA})_{22}$ NCs. (b) Isotope patterns of $[\text{Au}_{35}(\text{p-}o\text{-MBA})_{22}\text{-}2\text{H}]^{3-}$ species acquired experimentally (black curve) and theoretically (red curve). In Figure S35a, peak #1 corresponds to $[\text{Au}_{35}(\text{p-}o\text{-MBA})_{22}\text{-}2\text{H}]^{3-}$, and the other peaks (#2-#5) are from the successive coordination of $[+\text{Na} - \text{H}]$ of peak #1.

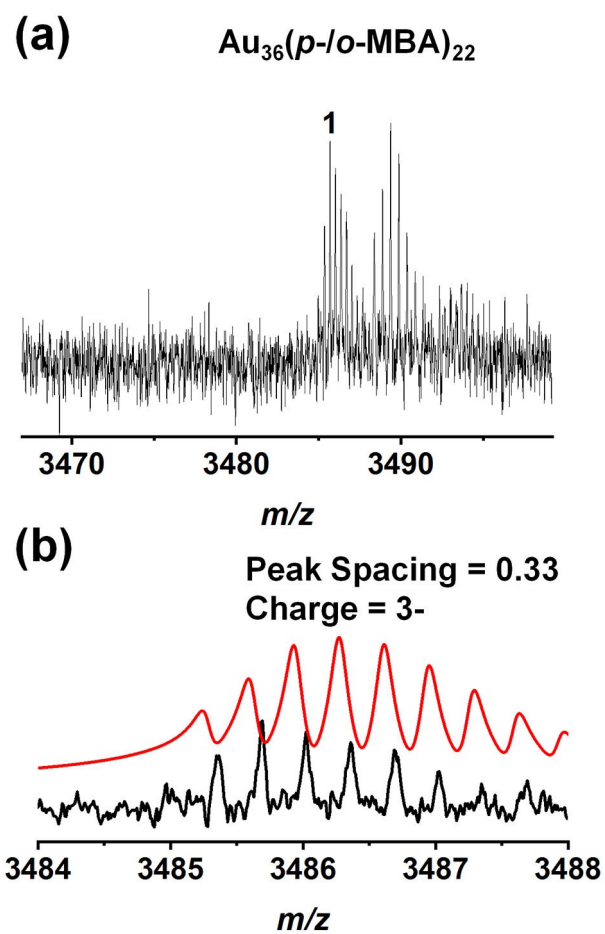


Figure S36. (a) Zoom-in ESI mass spectrum of the as-synthesized $\text{Au}_{36}(\text{p-}o\text{-MBA})_{22}$ NCs. (b) Isotope patterns of $[\text{Au}_{36}(\text{p-}o\text{-MBA})_{22}\text{-H}]^{3-}$ species acquired experimentally (black curve) and theoretically (red curve).

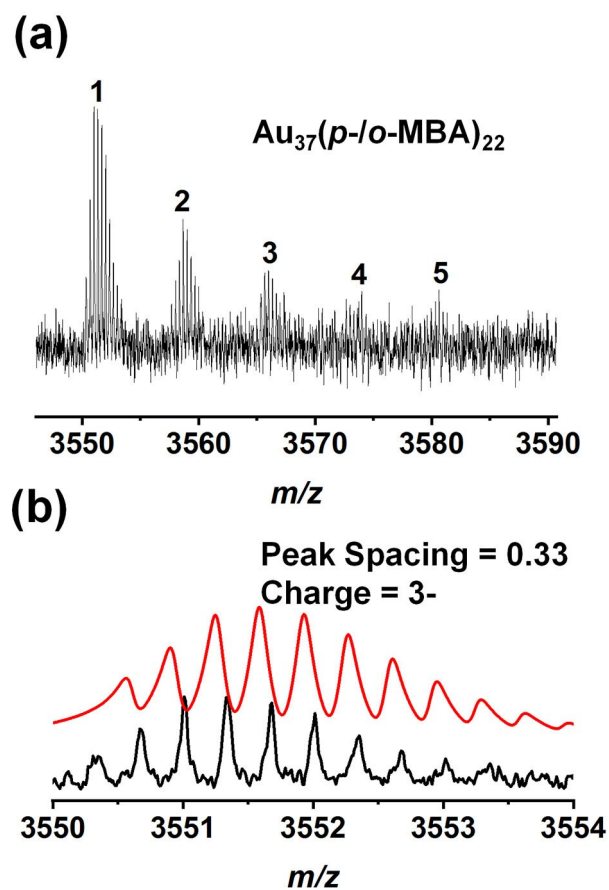


Figure S37. (a) Zoom-in ESI mass spectrum of the as-synthesized $\text{Au}_{37}(\text{p-}o\text{-MBA})_{22}$ NCs. (b) Isotope patterns of $[\text{Au}_{37}(\text{p-}o\text{-MBA})_{22}\text{-}2\text{H}]^{3-}$ species acquired experimentally (black curve) and theoretically (red curve). In Figure S37a, peak #1 corresponds to $[\text{Au}_{37}(\text{p-}o\text{-MBA})_{22}\text{-}2\text{H}]^{3-}$, and the other peaks (#2-#5) are from the successive coordination of [+ Na - H] of peak #1.

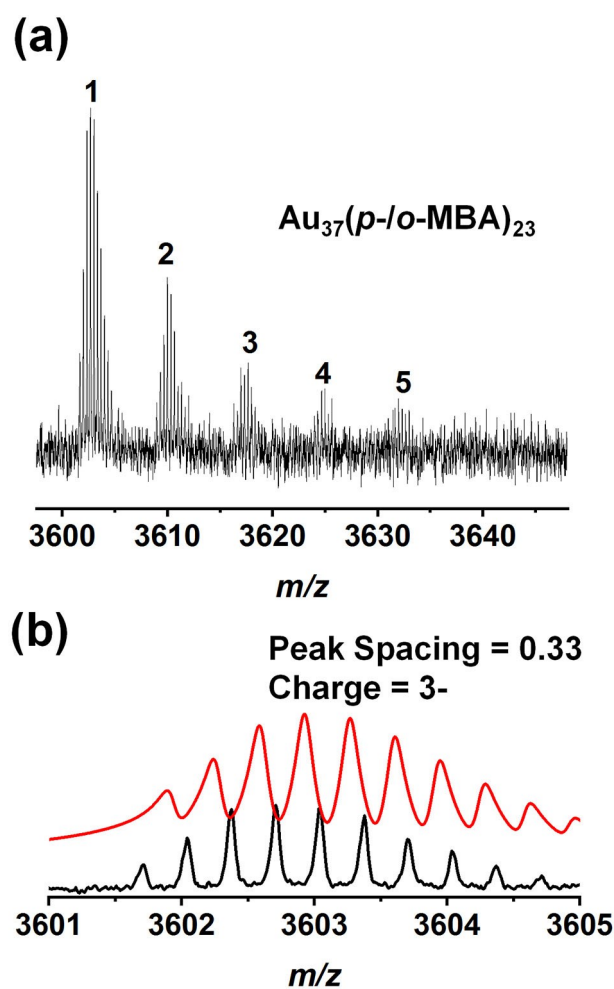


Figure S38. (a) Zoom-in ESI mass spectrum of the as-synthesized $\text{Au}_{37}(\text{p-}o\text{-MBA})_{23}$ NCs. (b) Isotope patterns of $[\text{Au}_{37}(\text{p-}o\text{-MBA})_{23}\text{-H}]^{3-}$ species acquired experimentally (black curve) and theoretically (red curve). In Figure S38a, peak #1 corresponds to $[\text{Au}_{37}(\text{p-}o\text{-MBA})_{23}\text{-H}]^{3-}$, and the other peaks (#2-#5) are from the successive coordination of $[+\text{Na} - \text{H}]$ of peak #1.

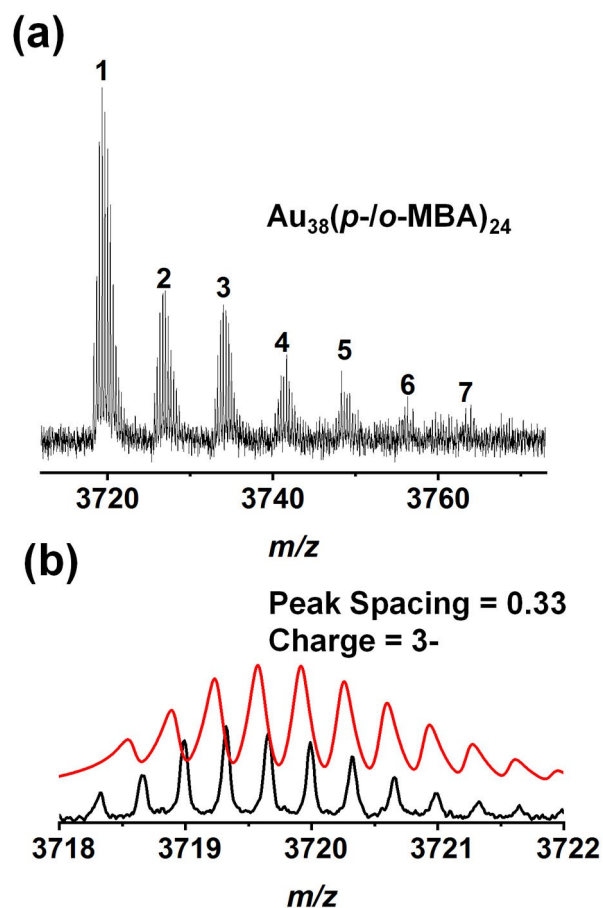


Figure S39. (a) Zoom-in ESI mass spectrum of the as-synthesized $\text{Au}_{38}(\text{p-}o\text{-MBA})_{24}$ NCs. (b) Isotope patterns of $[\text{Au}_{38}(\text{p-}o\text{-MBA})_{24}\text{-H}]^{3-}$ species acquired experimentally (black curve) and theoretically (red curve). In Figure S39a, peak #1 corresponds to $[\text{Au}_{38}(\text{p-}o\text{-MBA})_{24}\text{-H}]^{3-}$, and the other peaks (#2-#7) are from the successive coordination of $[+\text{Na} - \text{H}]$ of peak #1.

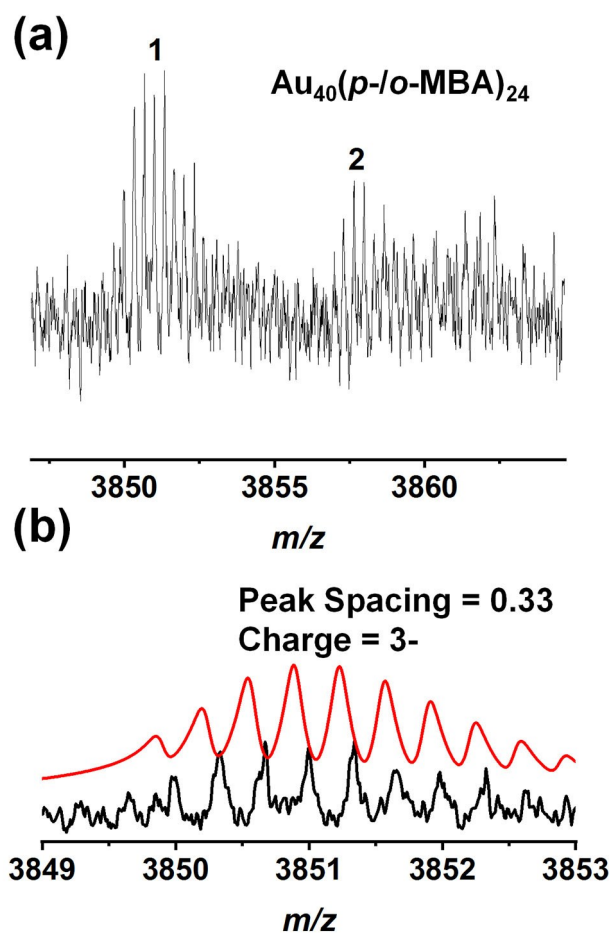


Figure S40. (a) Zoom-in ESI mass spectrum of the as-synthesized $\text{Au}_{40}(\text{p-}o\text{-MBA})_{24}$ NCs. (b) Isotope patterns of $[\text{Au}_{40}(\text{p-}o\text{-MBA})_{24}\text{-H}]^{3-}$ species acquired experimentally (black curve) and theoretically (red curve). In Figure S40a, peak #1 corresponds to $[\text{Au}_{40}(\text{p-}o\text{-MBA})_{24}\text{-H}]^{3-}$, and the other peak (#2) are from the successive coordination of $[+\text{Na} - \text{H}]$ of peak #1.

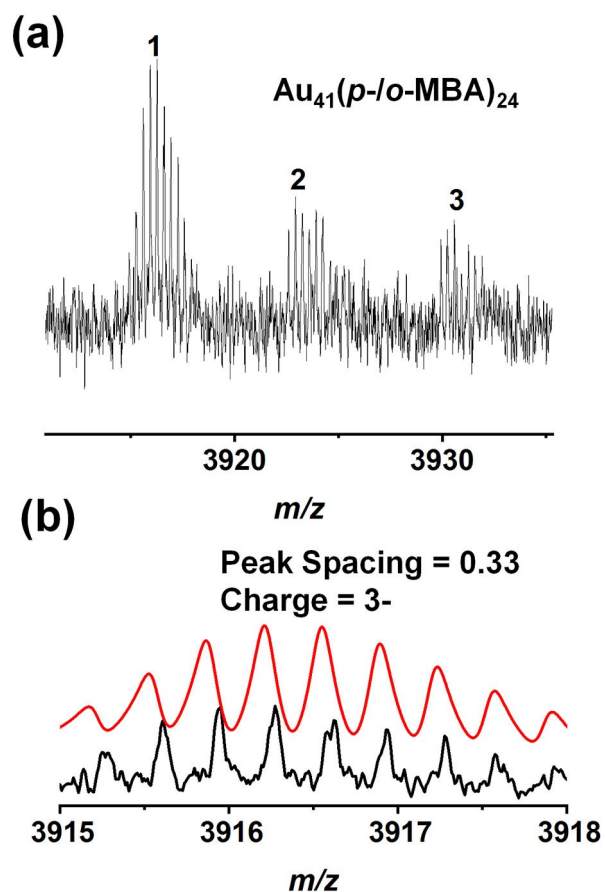


Figure S41. (a) Zoom-in ESI mass spectrum of the as-synthesized $\text{Au}_{41}(\text{p-}o\text{-MBA})_{24}$ NCs. (b) Isotope patterns of $[\text{Au}_{41}(\text{p-}o\text{-MBA})_{24}\text{-}2\text{H}]^{3-}$ species acquired experimentally (black curve) and theoretically (red curve). In Figure S41a, peak #1 corresponds to $[\text{Au}_{41}(\text{p-}o\text{-MBA})_{24}\text{-}2\text{H}]^{3-}$, and the other peaks (#2-#3) are from the successive coordination of $[\text{+ Na - H}]$ of peak #1.

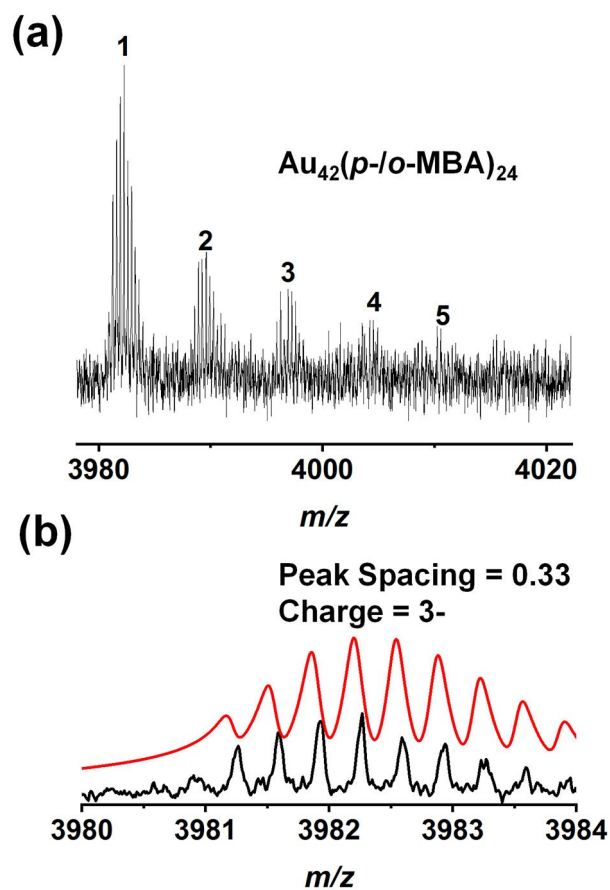


Figure S42. (a) Zoom-in ESI mass spectrum of the as-synthesized $\text{Au}_{42}(\text{p-}o\text{-MBA})_{24}$ NCs. (b) Isotope patterns of $[\text{Au}_{42}(\text{p-}o\text{-MBA})_{24}\text{-H}]^{3-}$ species acquired experimentally (black curve) and theoretically (red curve). In Figure S42a, peak #1 corresponds to $[\text{Au}_{42}(\text{p-}o\text{-MBA})_{24}\text{-H}]^{3-}$, and the other peaks (#2-#5) are from the successive coordination of [+ Na - H] of peak #1.

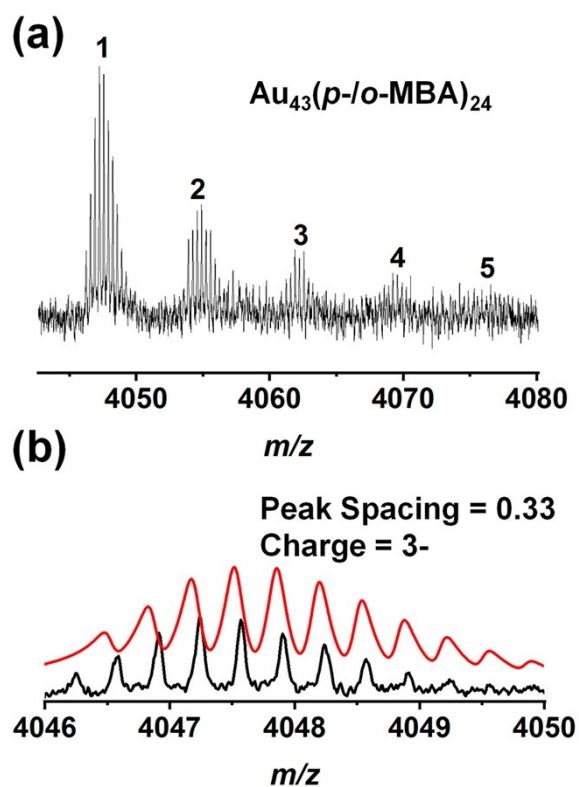


Figure S43. (a) Zoom-in ESI mass spectrum of the as-synthesized $\text{Au}_{43}(\text{p-}o\text{-MBA})_{24}$ NCs. (b) Isotope patterns of $[\text{Au}_{43}(\text{p-}o\text{-MBA})_{24}\text{-}2\text{H}]^{3-}$ species acquired experimentally (black curve) and theoretically (red curve). In Figure S43a, peak #1 corresponds to $[\text{Au}_{43}(\text{p-}o\text{-MBA})_{24}\text{-}2\text{H}]^{3-}$, and the other peaks (#2-#5) are from the successive coordination of $[+\text{Na} - \text{H}]$ of peak #1.

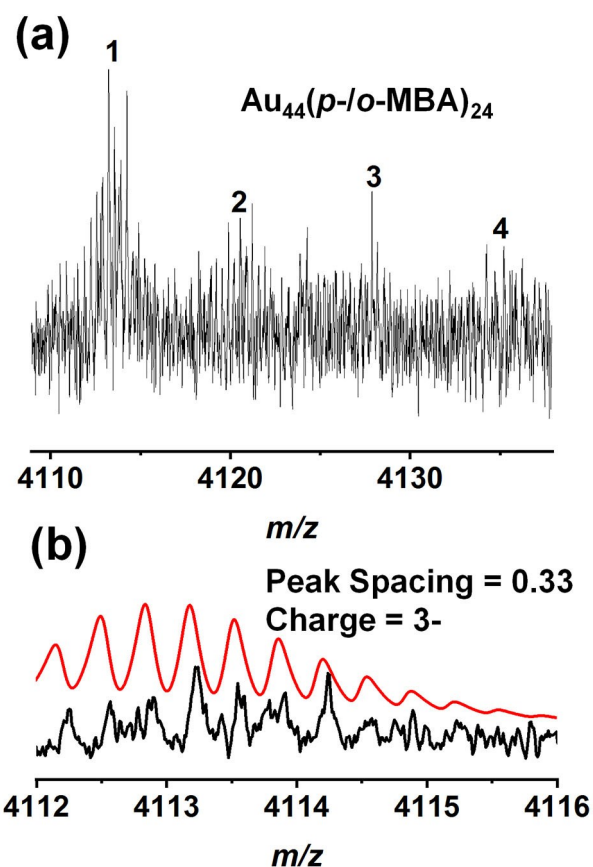


Figure S44. (a) Zoom-in ESI mass spectrum of the as-synthesized $\text{Au}_{44}(\text{p-}o\text{-MBA})_{24}$ NCs. (b) Isotope patterns of $[\text{Au}_{44}(\text{p-}o\text{-MBA})_{24}\text{-3H}]^{3-}$ species acquired experimentally (black curve) and theoretically (red curve). In Figure S44a, peak #1 corresponds to $[\text{Au}_{44}(\text{p-}o\text{-MBA})_{24}\text{-3H}]^{3-}$, and the other peaks (#2-#4) are from the successive coordination of [+ Na - H] of peak #1.

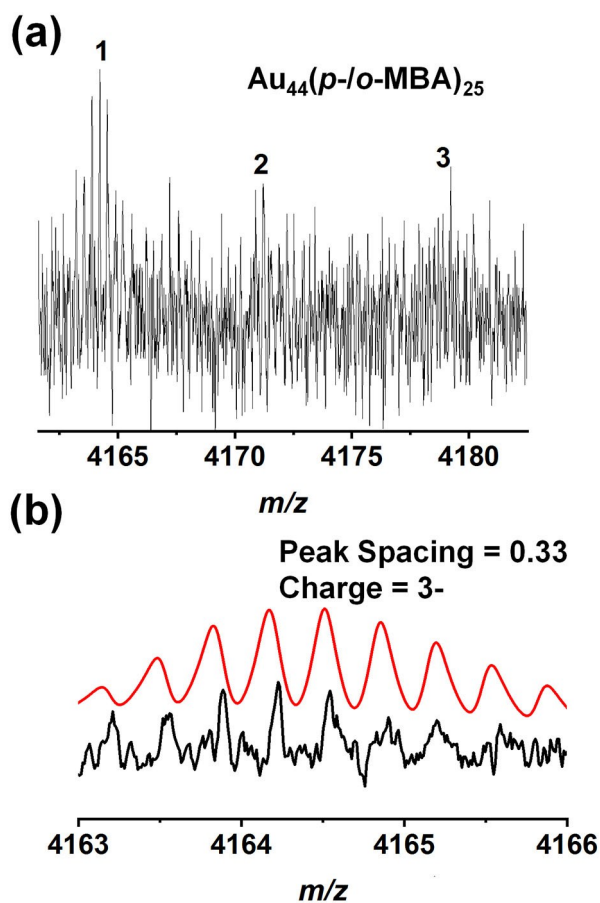


Figure S45. (a) Zoom-in ESI mass spectrum of the as-synthesized $\text{Au}_{44}(\text{p-}o\text{-MBA})_{25}$ NCs. (b) Isotope patterns of $[\text{Au}_{44}(\text{p-}o\text{-MBA})_{25}\text{-}2\text{H}]^{3-}$ species acquired experimentally (black curve) and theoretically (red curve). In Figure S45a, peak #1 corresponds to $[\text{Au}_{44}(\text{p-}o\text{-MBA})_{25}\text{-}2\text{H}]^{3-}$, and the other peaks (#2-#3) are from the successive coordination of $[\text{+ Na - H}]$ of peak #1.

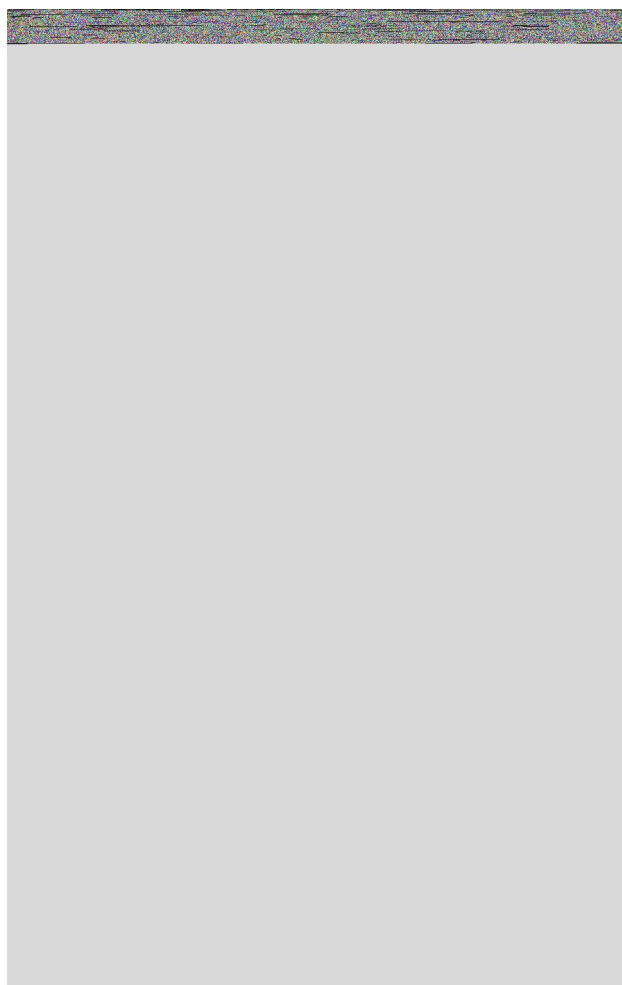


Figure S46. (a) Zoom-in ESI mass spectrum of the as-synthesized $\text{Au}_{44}(\text{p-}/\text{o-MBA})_{26}$ NCs. (b) Isotope patterns of $[\text{Au}_{44}(\text{p-}/\text{o-MBA})_{26}\text{-H}]^{3-}$ species acquired experimentally (black curve) and theoretically (red curve). In Figure S46a, peak #1 corresponds to $[\text{Au}_{44}(\text{p-}/\text{o-MBA})_{26}\text{-H}]^{3-}$, and the other peaks (#2-#3) are from the successive coordination of $[+\text{Na} - \text{H}]$ of peak #1.

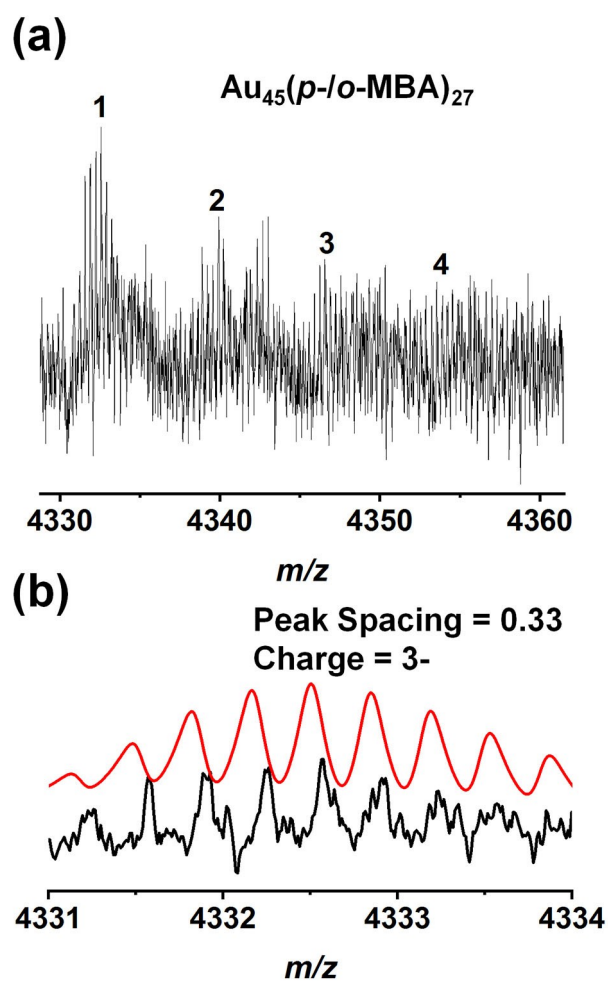


Figure S47. (a) Zoom-in ESI mass spectrum of the as-synthesized $\text{Au}_{45}(\text{p-}o\text{-MBA})_{27}$ NCs. (b) Isotope patterns of $[\text{Au}_{45}(\text{p-}o\text{-MBA})_{27}\text{-H}]^{3-}$ species acquired experimentally (black curve) and theoretically (red curve). In Figure S47a, peak #1 corresponds to $[\text{Au}_{45}(\text{p-}o\text{-MBA})_{27}\text{-H}]^{3-}$, and the other peaks (#2-#4) are from the successive coordination of $[+\text{Na} - \text{H}]$ of peak #1.